Control Engineering Practice 92 (2019) 104138

Contents lists available at ScienceDirect

Control Engineering Practice

journal homepage: www.elsevier.com/locate/conengprac

Mathematical modeling of Electric vehicles - A survey

Lekshmi S. *, Lal Priya P.S.

Department of Electrical Engineering, College of Engineering Trivandrum, Kerala, India

ARTICLE INFO

Keywords:
Electric vehicle model
Bicycle model
Brake model
Battery model
Tire model
Wheel dynamics

ABSTRACT

The paper presents a survey of the existing mathematical models of electric vehicles followed by state of the art approaches on modeling hybridization of the energy sources. The mathematical representation of the electric vehicle (EV) ranging from the simple single Degree of Freedom (DOF) models to complex multi-body dynamic models is discussed in detail. Reduced dynamic models applicable to various control design diligence are discussed which facilitates the selection of the optimal model for design. In addition to vehicle dynamics, the paper consolidates dynamic models of the different components of an electric vehicle including the transmission, brake, battery, wheel and tire dynamics. Comparative analysis of different versions of the models for each component is also presented, focusing on their application in controller design. The paper thus acts as a guide for any EV control design requirement, providing optimal models for particular applications.

1. Introduction

Electric Vehicles (EVs) have undoubtedly been proven to be the most viable environmentally friendly alternative to conventional vehicles and have gained significant acceptance in today's market. The recent advances in the electric vehicle domain are dominated by various control realizations. The major research is oriented in the direction of realizing various control requirements like — Traction Control (Aligia, Magallan, & Angelo, 2018), Fault-Tolerant Control (Wang, Yu, Yuan, & Chen, 2018), Trajectory Following Control (Guo, Luo, & Li, 2018), Longitudinal and Lateral Motion Control (Dai, Luo, & Li, 2013), and much more. As the initial step, every design process calls for prediction of the vehicle handling behavior and assessment optimization, where software simulations play a pivotal role. The accuracy of a simulation attempt depends greatly on the accurate mathematical portrayal of the vehicle handling dynamics. From the controller design perspective, the model should be simple enough enabling smooth implantation of model-based controllers yet capable of incarcerating the elementary dynamics. Also, the developed model has to exhibit adequate reliability, thereby minimizing the jeopardy and expense during experimental procedures, simultaneously aiding performance evaluation in the simulation.

1.1. Fundamental vehicle models

A wide range of mathematical descriptions of the vehicle dynamics is available in the literature, differing in the complexity of the models with different degrees of freedom. The basic dynamic models formulated from fundamentals of physics can accurately represent the force and moment dynamics mathematically (Ehsani, 2013). However, in case of critical vehicle handling maneuvers, it is vital to consider a more descriptive model considering the cross-coupling effects between various vehicle sub-components, kinematic constraints as well as geometrical non-linearities. The application of multi-body dynamics for the analysis of vehicle handling problems was initiated by McHenry (1969) which was later succeeded by several complex multibody dynamics models (Blundell, 1999, 2000). Kortm (1993) introduced a complete multi-body model of the vehicle inclusive of the suspension geometry and tire characteristics based on the SAE (Society of Automotive Engineers) frame of reference. Simultaneously several multi DOF non-linear multi-body dynamic models, that can accurately represent almost all physical characteristics of the vehicle including suspension and tire dynamics has been proposed (Hegazy, Rahnejat, & Hussain, 1999; Shabana, 2009). However, they are arduous in computation and as an attempt to scale down the computational burden, an intermediate multi-body model was proposed by Jaiswal, Mavros, Rahnejat, and King (2007), which was well accepted for less critical analysis requirements.

1.2. Simpler models for control design

However, whilst designing simpler control requirements these bulky models are rarely used in their raw form, owing to the inherent complexity in analysis and design. The complex mathematical form of the multi-body models demand a simultaneous solution of the combined differential and/or algebraic system of equations, thus introducing convergences issues with an increased computational burden. A great

* Corresponding author.
E-mail addresses: lekshmi.eee@gmail.com (S. Lekshmi), lalpriyaps@cet.ac.in (P.S. Lal Priya).

https://doi.org/10.1016/j.conengprac.2019.104138
Received 12 February 2019; Received in revised form 29 August 2019; Accepted 30 August 2019
Available online xxxx

amount of vehicle control systems, for instance, the side slip control, yaw control, and trajectory control utilizes a linearized version of vehicle operating condition known as the bicycle model (Norouzi, Kazemi, & Azadi, 2017). Here the vehicle is considered in its most simplified form, neglecting tire's lateral sliding, steering angles and assuming constant longitudinal velocity. These simplifications come at the cost of reduced accuracy in the model predicted responses as compared with actual vehicle responses. Also, neglecting the nonlinear tire dynamics and vehicle dynamics associated dynamic load transfer, accurate representation of actual vehicle behavior during severe maneuvers becomes difficult. A superior, nonlinear model reflecting the non-linear behavior of the tire is introduced in Liu, Ren, Chen, and Wang (2013), which makes use of piece-wise linearization of the tire dynamics to form 3 DOF bicycle nonlinear model.

All the control-oriented vehicle models can be used for simulation studies performed during vehicle design or performance analysis. The studies can be facilitated by use of forward simulation, which involves a feedback loop or employing the computationally simpler backward simulation. Backward simulation models are often used in vehicle control design for optimized component sizing corresponding to the speed–torque requirements (Shankar, Marco, & Carroll, 2011).

1.3. Modeling of EV components

By using any of the aforementioned techniques, accurate representation of vehicle motion dynamics can be obtained in the desired level of complexity. Modeling the complete characteristics of the vehicle requires an accurate representation of the characteristics of all physical parts of the vehicle namely — transmission, suspension, wheel–tire dynamics and brakes. The disposable peak torque from the power source with the granted driveline gear ratios determines the maximal force available for traction. Accurate knowledge of the vehicle power source as well as the transmission characteristics may come handy in the design of traction controllers. Traction control targets a reduction or elimination of inordinate slipping during acceleration thereby enhancing the controllability of the vehicle. This calls for an elaborate description of the frictional force dynamics at the tire–road interface (Automotive Stability Enhancement Systems, 2004). In de Wit and Tsiotras (1999) a lucubrate formulation of the frictional force dynamics representing the tire and road interactions, formulated based on the LuGre model (Wang et al., 2018) is presented. Whereas, the implementation and design of the ABS — Anti locking Brake System, that acts during braking to prevent the wheel locking, requires accurate representations of the tire transient behavior (Bakker, Nyborg, & Pacejka, 1987; Bakker, Pacejka, & Lidner, 1989).

1.4. Modeling alternate configurations of EV

With the advances in technology, various alternate configurations of EV is being used extensively nowadays, which elicit inclusion of modifications in wheel structure as well as power train. The idea of using In-Wheel Motors(INW) instead of a centralized drive, is gaining increased acceptance owing to its many advantages, like the minimized mass of the vehicle, thereby improving the onboard battery storage capacity of the vehicle. The increasing use of INWs calls for an accurate model of the in-wheel system for control design applications. A variety of in-wheel motor systems in use differ in the choice of motor, of which the permanent magnet synchronous motors (PMSMs) are used commonly (Pop & Fodorean, 2016; Suh, Hwang, Lee, & Kim, 2013). Switched Reluctance Motors (SRM) are slowly becoming a favorite choice owing to its higher initial torque for rapid acceleration, higher efficiency reducing the energy consumption and a wide operating speed range (Luk & Jinupun, 2006). However, the noticeable noise and vibration effects caused by the labile radial force in SRM overshadow the inherent advantages, which calls for proper research on vibration analysis and control (Sun, Li, Huang, & Zhang, 2015; Wang, Li, & Ren, 2016).

Several modified versions of the electric vehicle have been formulated recently, introducing variations in the power source. A variety of models for representing the battery characteristics of an EV, from the simple voltage source model to the complex nonlinear models are available in the literature (Chan, 2000; Dowgiallo, 1980; Salameh, Casacca, & Lynch, 1992). Owing to its limitation of having constricted range for battery-powered EV, researchers are looking for an alternative which makes use of the fuel cells as energy sources. There are fuel cell-powered hybrid EVs, where the fuel cells are used to supplement the power from the battery. Various configurations of fuel cell technologies (Wood, Wang, Gonder, & Ulsh, 2013) have been put forward which utilizes a variety of fuels, hydrogen as well as liquid fuels such as methanol, ethanol and also methane (Graves, Ebbesen, Mogensen, & Lackner, 2011; Jensen, Sun, Ebbesen, Knibbe, & Mogensen, 2010). The Fuel cell Range Extended Electric Vehicles(FCREEV) is one of the latest solutions for improving the limited range issue of EVs, maintaining the zero-emission capability (Mller, Bernt, Salman, & Trattner, 2017).

1.5. About the paper

This survey is an attempt to consolidate the available models of EVs, acquainting models varying in complexity and content. The paper can act as a guiding light for the control engineers working on analysis and/or the design process in the field of EV. Beginning with the basic mathematical representations derived from the principles of physics, the paper presents the models available for different control requirements. Often, the models used in control design neglects the complex dynamics of various physical components of the vehicle. Here, the mathematical models of all the basic components of the electric vehicle are discussed — namely the transmission, brake, wheel and tire dynamics, battery and fuel cell. The available configurations ranging from the most simple dynamics suitable for less critical control designs to the most complex models involving all aspects of the vehicle dynamics are also included.

This paper is aimed at facilitating design works in the control engineering domain. EV models are also widely used in various other engineering design domains such as EV-grid interfacing power flow analysis and energy management systems. To analyze the impact of EV charging systems on the power grid, several EV load models have been developed (Haidar & Muttaqi, 2015). Based on the power model from state of charge (SOC) of the battery, plug-in EV models are formulated in Jimenez and Garcia (2011) for power flow studies. A more useful EV load model for simulation study is discussed in Kongjeen and Bhumkittipich (2016), where user-defined modeling methods for power system analysis toolbox are presented. However, this survey is limited to the EV models formulated for the control domain and EV models formulated for other domains, such as in power distribution and power flow analysis are not considered in this survey.

1.6. Highlights of the paper

- The paper is first of its kind that summaries the available EV mathematical models, as applicable for any EV control design project.
- Starting with the basic dynamic model, various versions of the vehicular models are presented, ranging from the simplest bicycle model to the most complex multi-body model.
- The versions of mathematical models of all the physical components namely — transmission, brakes, batteries, tire dynamics are compiled together which can facilitate the selection of an optimal model for the particular purpose.
- A comparative analysis of available battery models as well the fuel cell models is done, along with a detailed description of the most accurate models.
- The paper can usher EV control design projects, providing apposite mathematical representations of all the EV components that best fit design requirements.

The survey is structured as follows. The EV power train and its basic components are briefly explained in Section 2. Section 3 discusses the fundamental vehicle models followed by the simpler models for control design in Section 4. Sections 5 and 6 present the transmission and wheel dynamics respectively. Various aspects of the tire modeling stating different available tire models are presented in Section 7. Section 8 explains the INW electric vehicle model, followed by various brake models in Section 9. The battery models and fuel cell models are given in Sections 10 and 11 respectively. Section 12 wraps up the survey with conclusions and discussions.

2. The electric vehicle power train

Various architectures of the electric vehicle exist, because of the numerous possibilities available for reconfiguration of components from the choice of electric machines, selection of battery voltage and recharging configuration, inclusion or exclusion of gearbox, etc. (Soylu, 2011). There can be a centralized electric motor drive or further use a four in-wheel electric drive, which can provide better maneuverability. The energy source can be modified to include auxiliary power for increasing the driving range in the form of fuel cells, supercapacitors, etc or can be remodeled as a hybrid vehicle incorporating an IC engine.

The basic components of an electric vehicle power train can be formulated as shown in Fig. 1. The battery power-driven electric machine drives the vehicle by delivering the traction power of the wheels. The torque generated by the traction motor is conveyed to the wheels through the transmission consisting of clutch, gearbox, differential, and driveshaft. The gear selection can be avoided in EV, by choosing an electric machine whose characteristics closely match with the driving torque–speed requirements. The electric machines speed and torque are controlled by the power electronics designed suitably. Auxiliary loads account for the loss components that are excluded from the main power train from the power source to the driven wheels like the lighting, comfort and safety systems incorporated into the vehicle. A braking resistor is included to keep a check on the maximum voltage of the battery during regenerative braking. The plugin versions use grid connectivity to recharge the battery where a rectifier and boost converter is used to ensure adequate voltage coupling.

3. Fundamental vehicle modeling

3.1. Introduction

Modeling of an electric vehicle begins with the formulation of the basic dynamics of a general vehicle. Vehicle behavior can be mathematically described based on the fundamental principles of physics. To represent a vehicle, which is a very complex system with numerous subsystems, calls for sophisticated mechanical and mathematical knowledge. The following Sections describes the fundamental vehicle models formulated from the first principles of mechanics. The fundamental vehicle dynamic models discussed below are general to any four-wheel vehicle. This can very well be used to represent the EV with appropriate add ons to represent other components in the power train, which are discussed in the following Sections.

3.2. Kinematic model

The fundamental vehicle dynamic model can be developed by the application of fundamental principles of mechanics, especially Newton's laws of motion. Inspection of the forces acting along the direction of the velocity on the vehicle body can completely describe the vehicle state (Ehsani, 2013). The movement of the vehicle up a grade is considered for formulating the dynamic model; the forces appearing along the vehicle body are given in Fig. 2.

The major external forces on the body of vehicle along longitudinal direction, are -(i) the forward tractive effort $\overrightarrow{F_t}$, in the adjoin area between driven wheel tires and (ii) the road surface and the retarding resistive forces such as the front and rear tires rolling resistance represented with rolling resistance moment $\overrightarrow{F_r}$, aerodynamic drag $\overrightarrow{F_w}$ and grading resistance $\overrightarrow{F_g}$.

(*Suffixes 'f' and 'r' are used to represent the vectors corresponding to front and rear wheels.*)

The dynamic equation of the vehicle with mass M moving along the longitudinal direction with velocity $\overrightarrow{V}$ can be obtained as in (1).

$$M\frac{d\overrightarrow{V}}{dt} = (\overrightarrow{F_{tf}} + \overrightarrow{F_{tr}}) - (\overrightarrow{F_{rr}} + \overrightarrow{F_{rf}} + \overrightarrow{F_w} + \overrightarrow{F_g}) \tag{1}$$

Tractive forces $\overrightarrow{F_{tf}}$ and $\overrightarrow{F_{tr}}$ are positive, when the direction of vehicle velocity is forward and negative when the velocity is in reverse direction.

Definition 3.1. Rolling resistance moments $\overrightarrow{T_{rf}}$ and $\overrightarrow{T_{rr}}$ are the generated due to the resistance offered by tires when running on hard surfaces, due to the unsymmetrical ground reaction force distribution caused by hysteresis in the tire materials. In order to balance this moment and keep the wheel rolling, reaction forces $\overrightarrow{F_{rf}}$ and $\overrightarrow{F_{rr}}$ acts on the center of the wheel, opposing the tractive force $\overrightarrow{F_t}$ which is acting along the direction of motion (Ehsani, 2013). The rolling reaction force can be expressed as given in (2).

$$\overrightarrow{F_r} = Mgf_r cos\alpha \quad \cdot \frac{\overrightarrow{V}}{|V|} \tag{2}$$

where f_r is the rolling resistance coefficient, which depends on the tire material and its physical properties and α is the road angle in radians. g is acceleration due to gravity.

Definition 3.2. Aerodynamic drag is the resistive force acted upon a vehicle gushing at a specific velocity in air, opposing the direction of motion. It can be expressed in terms of the vehicle velocity $\overrightarrow{V}$, the frontal area of the vehicle A_f, and air density ρ as Ehsani (2013) as in (3).

$$\overrightarrow{F_w} = \frac{1}{2}\rho A_f C_D(\overrightarrow{V} + \overrightarrow{V_w})^2 \cdot \frac{\overrightarrow{(V + V_w)}}{|(V + V_w)|} \tag{3}$$

where V_w is the wind velocity and C_D is the aerodynamic drag coefficient that characterizes the shape of the vehicle.

Definition 3.3. The grading force produced by the weight of the vehicle, when a vehicle moves up/down a slope, is called grading resistance. This force which always acts along the gravity in the downward direction with a component opposing the tractive force can be expressed as in (4).

$$\overrightarrow{F_v} = Mgsin\alpha \tag{4}$$

The tractive effort acting on the driven wheels through the power train is limited by the tire–ground cohesion. For stable vehicle control, the tractive force should not exceed the maximum tractive force F_{tmax} as ascertained by W, the normal load and μ, the road adherence coefficient.

$$F_{tmax} = \mu.W \tag{5}$$

The load acting normal on the front and rear wheels W_f,W_r can be obtained as the resultant of the force moments about the center of tire–road contact area as shown in (6) and (7).

$$\overrightarrow{W_f} = \frac{L_b}{L}M_g cos\alpha - \frac{h_g}{L}[\overrightarrow{F_t} - \overrightarrow{F_r}(1 - \frac{r_d y}{h_g})] \tag{6}$$

$$\overrightarrow{W_r} = \frac{L_a}{L}M_g cos\alpha + \frac{h_g}{L}[\overrightarrow{F_t} - \overrightarrow{F_r}(1 - \frac{r_d y}{h_g})] \tag{7}$$

where, r_{dy} is the dynamic resistance of the tire, L_a, L_b, L, h_g are lengths and height respectively with reference to Fig. 2.

As seen from (5), the main limiting value for the tractive force acting on the wheel is the adhesive capacity between the tire and the ground

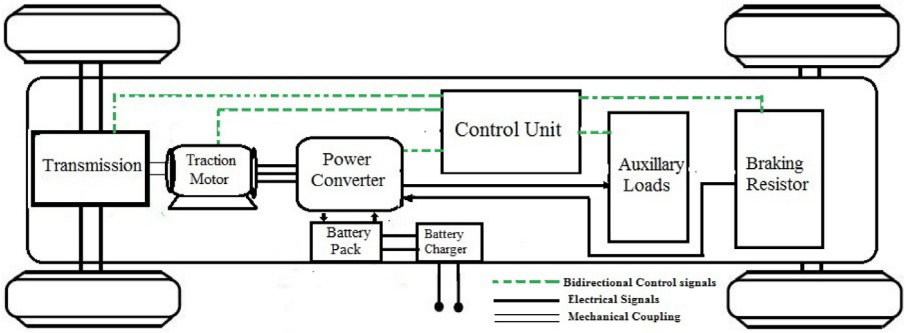

Fig. 1. Electric vehicle power train.

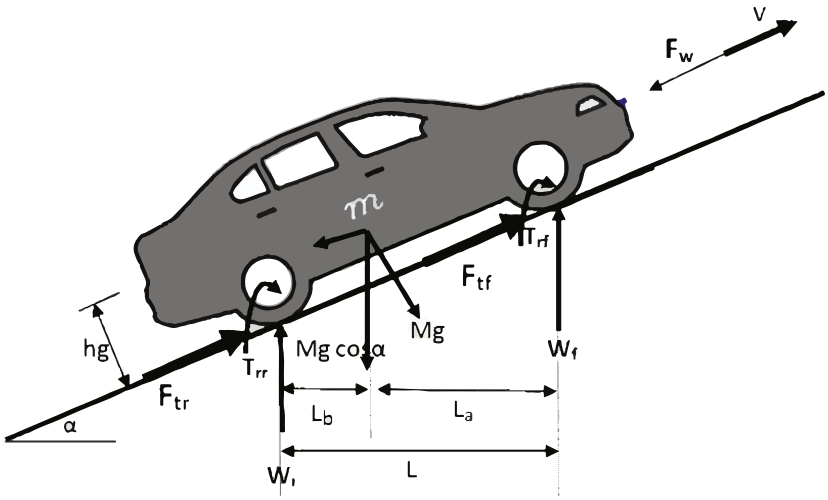

Fig. 2. Forces appearing on the vehicle body.

and not the maximum torque the engine can supply. Experimental results on different types of roads also backs the fact that the maximum traction force applicable on the drive wheel depends highly on the slipping of the driven wheel. The slip or relative motion between the tires and the road can be written as in (8) and (9).

Driving slip,

$$S = (1 - \frac{V_t}{r.\omega}) \times 100\% \quad = (1 - \frac{r_e}{r}) \times 100\% \tag{8}$$

Braking slip,

$$S = (1 - \frac{r.\omega}{V_t}) \times 100\% = (1 - \frac{r}{r_e}) \times 100\% \tag{9}$$

V_t is the tire center translatory speed, ω, the tire angular speed, r and r_e are the free rolling tire's rolling radius and effective tire rolling radius.

Specific values of various vehicle or road depended values for different vehicles and surfaces are provided in Ehsani (2013), which can be used to select suitable values during design.

3.3. Four wheel drive planar dynamic model

The fundamental dynamic model for a vehicle discussed in the previous section considers the uphill motion of the vehicle. During control design problems, it is often easier to consider a planar or horizontal motion of the vehicle. A detailed kinematic model for a four wheel drive electric vehicle on a planar and horizontal road, considering longitudinal and lateral dynamics is presented in Suh et al. (2013). As given in Fig. 3, the dynamics of the vehicle can be described using moving coordinates of x, y and z for longitudinal, lateral and vertical motions of its center of gravity, ϕ_Y and ϕ_R are the body yaw and roll angle. The guidance input for the front wheels generate the individual wheel forces which are expressed in the wheel frame.

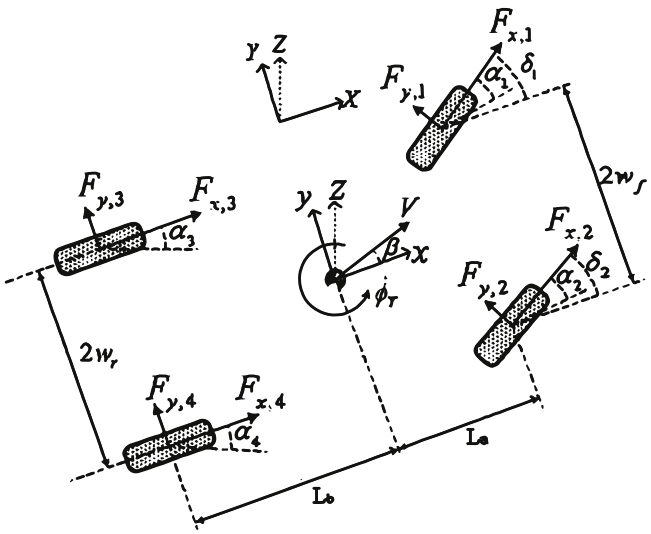

Fig. 3. Four wheel planar kinematic model.

The longitudinal and lateral accelerations a_x, a_y can be formulated with Newton's law on the inertial frame and can be obtained in terms of components of forces in Fig. 3 as given in (10) and (11).

$$a_x = 1/M(F_{x1}cos\delta_1 + F_{x2}cos\delta_2 - F_{y1}sin\delta_1 - F_{y2}sin\delta_2 + F_{x3} + F_{x4}) \quad (10)$$

$$a_y = 1/M(F_{x1}sin\delta_1 + F_{x2}sin\delta_2 - F_{y1}cos\delta_1 - F_{y2}cos\delta_2 + F_{y3} + F_{y4}) \quad (11)$$

The yaw rate on the inertial frame can be obtained from the rotational equivalent of Newton's law as in (12).

$$I(\phi_r) = L_a(F_{y1}cos\delta_1 + F_{y2}cos\delta_2 + F_{x1}sin\delta_1 + F_{x2}sin\delta_2) - L_b(F_{y3} + F_{y4}) + w_f(F_{y1}sin\delta_1 - F_{y2}sin\delta_2 - F_{x1}cos\delta_1 + F_{x2}cos\delta_2)w_f(F_{x3} + F_{x4}) \quad (12)$$

L_a, L_b, w_f, w_r are dimensions of the vehicle as given in Fig. 3. Also, the longitudinal and lateral accelerations in the inertial reference frame can be expressed in terms of derivatives of the vehicle body accelerations V_x and V_y. It should not be neglected that the vehicle longitudinal and lateral velocities are coupled and proper decoupling steps are to be applied.

The explicit relations between the forces at the wheels and the variables that describe the motion are found by using wheel rotational dynamics model. The translational speed of the center of each wheel with reference to the body center of gravity can be described as given in (13)–(16), using the vehicle body longitudinal and lateral velocity (V_x, V_y) and $(\dot{\phi_y})$, the yaw rate.

$$V_{t1} = (V_x - w_f\dot{\phi_y})cos\delta_1 + (V_y + L_a\dot{\phi_y})sin\delta_1 \quad (13)$$

$$V_{t2} = (V_x - w_f\dot{\phi_y})cos\delta_2 + (V_y + L_a\dot{\phi_y})sin\delta_2 \quad (14)$$

$$V_{t3} = (V_x - w_f\dot{\phi_y}) \quad (15)$$

$$V_{t3} = (V_x + w_f\dot{\phi_y}) \quad (16)$$

Using kinematics and geometry, the vehicle body slip angle (β) and side slip angle (α) of each wheel can be computed (Suh et al., 2013).

These relationships can be used for formulating the state-space model which will can be used for controller design.

3.4. Multi-body dynamic model

For analysis of basic vehicle handling behavior and stability of vehicle, the simple dynamic models discussed in previous Sections can be used. However, when used for design or analysis of critical handling maneuvers, a detailed model which also considers the suspension geometry and tire characteristics effects on the handling behavior will be better suited. For similar iterative design optimization process, the multi-body vehicle modeling approach will serve as a better option. The multi-body dynamics vehicle models reflects the characteristics of all couplings that exist between several subsystems in the vehicle along with the different non linearities and types of kinematic constraints.

The multi-body modeling process assigns a reference frame and six DOF to each of the vehicle rigid-body components. The formulation of the model is primarily done using the constrained Lagrange equation, where the reaction forces limited by the constraints are calculated as the Lagrange multipliers. The combined system of equations are solved considering the constrained Lagrange equations for all potential DOF within the system.

A non-linear multi DOF multi-body dynamics model of a vehicle is presented in Hegazy et al. (1999), comprising of front suspensions and steering system, rear double-wishbone suspensions and vehicle inertia. A fixed global reference frame - X, Y, Z is used to describe vehicle motion and each moving part i is attached with a local part reference frame - x_i, y_i, z_i. The equations of motions for each part of the vehicle body is formulated by using a generic method based upon constrained systems Lagrange's equation as:

The set of differential equations representing the vehicle motion and the applied forces like tire forces, bushing reactions are solved to determine, the system state variables and the Lagrange model for the joint's reactions. The set of equations is depicted by the matrix equation given in (17).

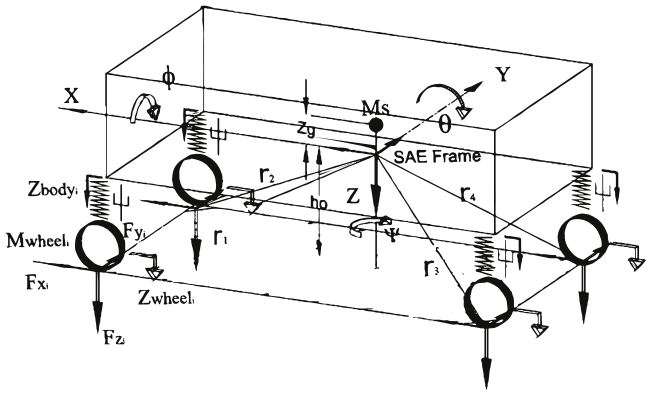

Fig. 4. SAE frame of reference and vehicle model (Jaiswal et al., 2007).

$$[J](q, \lambda)^T = (F_q) \quad (17)$$

where:

$$J = \begin{bmatrix} \left[\frac{s}{dt}\frac{\partial K}{\partial q} + \frac{\partial K}{\partial q}\right] & \frac{\partial C}{\partial \lambda} \\ \frac{\partial C}{\partial q} & 0 \end{bmatrix}$$

Although this model accurately incorporates the dynamics of the vehicle, the computational effort required, as in the case of any approach supported by the constrained Lagrange equation, is high. Thus it is advisable to choose relatively simpler models for less critical analysis requirements. The following Section describes an intermediate multi body model with dynamic equations formulated using Newton–Euler method of derivation, which can be utilized for the simulation of handling dynamics of the vehicle.

3.5. Intermediate multi-body model

An intermediate multi body model of the electric vehicle, formulated from the dynamic equations by using Newton–Euler formulation for the study of critical maneuvering is presented in Jaiswal et al. (2007). The Newton–Euler approach is much accepted owing to its accuracy and also the lesser computational effort required than other methods based on the constrained Lagrange equation. However, the modeling by this approach considers certain assumptions or simplifications which make it less applicable to situations with rigorous handling operations directly implicating safety of passengers. Thus the selection between the Lagrange equation approach and Newton–Euler approach is a trade-off between accuracy and ease of computation process.

The comparatively simple configuration of intermediate models helps in identifying usual trends observed in relation with the parameters of the vehicle. This helps in drawing useful conclusions which are more difficult to obtain when using complex models with more interactions. The model presented in Jaiswal et al. (2007) has given extra attention in including the suspension property in a realistic way. This constitutes modeling of the suspension mechanisms and obtaining the rigid suspension reactions by applying virtual work approach.

The prime vehicle dynamics originate from the 6 motions in space corresponding to the sprung mass with respect to the mobile reference frame (Vehicle Dynamics Terminology, 2008), connected to the sprung vehicle body portion pursuing its 3 displacements and rotations in space. The method is in accordance with the common practice and has the advantage that the externally generated tire and aerodynamic forces can be easily defined in the local reference frame of vehicle, than in a global frame of reference. Also, as the results are offered as

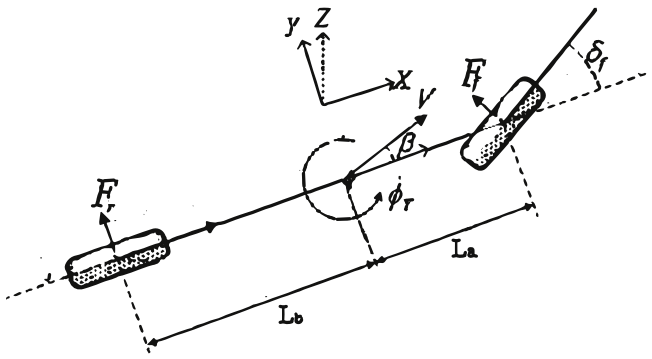

Fig. 5. Vehicle 2-DOF bicyle model.

displacements and velocities with respect to the vehicle, they are more useful.

The vehicle model is shown in Fig. 4, including the 4 unsprung and sprung mass, wheels and tires, as well as the parts of suspension. The 14 DOF model of the vehicle constitutes the complete 6 DOF sprung mass motion with the unsprung mass vertical movement, and an extra rotational DOF to include the wheel rotation about their spin axes (Jaiswal et al., 2007). The dynamic equations for the 3 translational and 3 rotational degree of freedom can be obtained as in Abe (2015).

The accuracy of the intermediate model was verified by comparison with experimental measurements carried out on an actual vehicle (Jaiswal et al., 2007). The model accuracy can be further increased by including factors like bump-steer and provision for steer and suspension compliance.

4. Control design oriented vehicle models

4.1. Introduction

The fundamental vehicle models presented in the previous Sections include all complex dynamics of the vehicle. The complexity of that degree is not required in simpler control design requirements. Simplified versions of the vehicle models are widely used in control design and analysis. One such simplified model known, the bicycle model along with its advanced nonlinear model is presented in the following Sections. Also, a 4 wheel drive vehicle model along with the trajectory following kinematics model is explained, which are designed for specific control applications. These models are equally applicable for representing general vehicle dynamics as well as for EV dynamics.

4.2. 2-DOF linear bicycle model

Bicycle model is one of the most frequently preferred form of vehicle representation, owing to its simplicity and lesser computational requirements. For control design requirements not requiring critical dynamics analysis, this simplified model is of great applications (Norouzi et al., 2017). The bicycle model as shown in the Fig. 5, has 2 DOF — yaw rate and lateral sliding angle.

The dynamic model has been formulated neglecting certain freedoms such as roll, bounce and pitch with following assumptions considered during the design:

1. Front and rear tires lateral sliding and steering angles are neglected.
2. It is assumptive that the longitudinal velocity remains constant with value taken between v_1 and v_2.
3. A linear relationship is assumed to exist between the lateral forces of tire and the sliding angle.

The dynamics of body slip angle (β) and yaw rate (ϕ'_y) representing the model can be obtained as a function of front (c_f) and rear (c_r) tire cornering stiffness and nominal lateral stiffness c* along with the front steering angle (δ_f) as in (18) and (19),

$$\beta' = (-2\frac{(c_f^* + c_r^*)}{MV_x})\beta + (-1 + 2\frac{(L_b c_r^* - L_a c_f^*)}{(MV_x^2)})\phi_y + 2(2\frac{c_f^*}{MV_x})\delta_f \tag{18}$$

$$\phi'_y = (2\frac{(L_b c_r^* - L_a c_f^*)}{J})\beta + (-2\frac{(c_f^* L_a^2 + c_r^* L_b^2)}{JV_x})\phi_y + (2\frac{L_a c_f^*}{J})\delta_f \tag{19}$$

The tire lateral forces in terms of friction coefficient μ are expressed as given in (20) and (21).

$$F_f = \alpha_f c_f^* = \alpha_f c_f \mu \tag{20}$$

$$F_r = \alpha_r c_r^* = \alpha_r c_r \mu \tag{21}$$

From the Fig. 5, based on the equations formulated by Rajamani (2011), the desired road yaw angle (ψ_d) can be expressed in terms of desired position coordinates X_{des}-Y_{des} as follows :

$$\psi_d = arctan\frac{Y'_{des}}{X'_{des}} \tag{22}$$

The final position coordinates can also be achieved in global coordinates as shown below in (23) and (24).

$$X = \int_0^t V_x cos\psi_d dt - e_1 sin\psi_d \tag{23}$$

$$Y = \int_0^t V_x sin\psi_d dt + e_1 cos\psi_d \tag{24}$$

where, V_x is the velocity and e_1 is the spacing of vehicle center of gravity (COG) from the origin. A state model of the vehicle has been presented, considering the lateral (y) and yaw vehicular motion depicting the linear characteristics of tire force with respect to slip angle (Liu et al., 2013).

In spite of the simplicity of the bicycle model, it is seldom used for intricate control designs because of certain limitations in those applications. The major fall back occurs due to the non-linear liaison of the lateral force of tires with its slip angle. The presence of tire force non-linear attributes, the linearized bicycle model predicted responses will vary considerably from the actual vehicle response. Thus when used for vehicle operations involving hefty lateral speeding, a nonlinear model reflecting the nonlinear attributes will be a better choice.

4.3. Non-linear bicycle model

A non-linear bicycle model considering the longitudinal (X), lateral (Y), and yaw (Φ_y) motion of the vehicle is discussed in Liu et al. (2013). The model is formulated with the assumption that the vehicle mass is completely in the vehicle rigid base. From Fig. 6, the dynamic equations for the nonlinear bicycle model can be obtained as shown in (25).

$$M(\dot{x} - yr) = \sum F_{xi}(i = f, r)$$
$$(\dot{y} - xr) = \sum F yi(i = f, r)$$
$$I_2\dot{\phi}_y = F_{yf} \cdot L_a - F_{yr} \cdot L_b \tag{25}$$

Here, F_{xi}, F_{yi} represent the forces along x, y-axis, which can be computed by the longitudinal F_{xwi} and lateral F_{ywi} tire force and the steer angle (δ) of the wheel. Considering the wheel dynamics discussed in Section 6, the rotational motion caused by applying driving torque T_d and braking torque T_b can be expressed in terms of the yaw moment of inertia (I_z), the effective tire radius (R_w) and the tire angular velocity (ω_w) as:

$$I_z\omega'_{wi} = T_{di} - F_{xi}R_w - T_{bi} \tag{26}$$

For application in vehicle stability control system synthesis, a state space representation of the nonlinear bicycle model is also available in discrete form Suh et al. (2013).

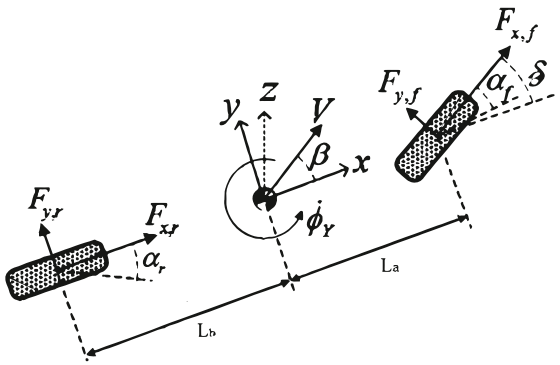

Fig. 6. Non linear 3 DOF bicycle model.

A detailed comparison of the vehicle responses of the linear and nonlinear bicycle models, a comparative analysis has been done in Ren, Shim, Ryu, and Chen (2014) with the CarSim model which is considered equivalent to a real vehicle. CarSim software finds wide application in the automotive industry for simulating vehicle dynamics. During lower speeds, linear as well as the nonlinear bicycle model trajectory twinned with the CarSim simulation response. However, on higher speeds, linear model trajectory varies significantly as compared to others, as anticipated because of neglecting the tire force saturation. But the nonlinear model trajectory is better harmonized with the CarSim results (Ren et al., 2014).

4.4. Four wheel steering vehicle model

As vehicle handling stability gained more attention related to vehicle safety, different options for improving the controllability of the vehicle became an interesting topic in the development of automobile industry. Four wheel steering (4WS) vehicles attracted much attention because of its inherent features like improved low speed maneuverability and enhanced high speed stability. The vehicle transient response can be improved by the participation of the rear wheels in steering process. A large number of control strategies are applied on 4WS vehicle and are available in literature. For proper design and analysis of control strategies an accurate model of 4WS featuring the characteristics related to stabilization in lateral and longitudinal domain of 4WS vehicle is required. A 3 DOF 4WS vehicle model is discussed in Yu, Wang, Wang, and Chen (2018) with a nonlinear tire model considering the crosswind disturbances.

The nonlinear model for a 4WS vehicle is formulated taking the vehicle COG as the body frame (x, y, z). Considering the 3 degree of freedoms — lateral, yaw and roll, the model can be formulated by representing the dynamics of the resultant of the external forces and moments (F_y, M_z and L_x) acting on the vehicle as follows:

$$\begin{aligned} \sum F_y &= Mv(\beta' + r) + m_s h_s \phi'' \\ \sum M_z &= I_z r' - I_{xz}\phi'' \\ \sum L_x &= I_x \phi'' - I_{xz} r' \end{aligned} \tag{27}$$

β and r are the side slip angle and the yaw rate of vehicle at COG, ϕ and ϕ' are roll angle and velocity, I_x is the roll moment of inertia, I_z is the yaw inertia moment, I_xz is the product of inertia about x and z axes. So as to ease the implementation of the control strategy, a relatively simpler 2 DOF vehicle model is also formulated containing only the side slip and yaw rate considering most of the applicable dynamics. The simplified 2 DOF model, very similar to the bicycle model is given in Yu et al. (2018), with the coordinate frame at the COG of the vehicle. Detailed model considering the influence of the crosswind along with the state model of the linear 2 DOF model is also available in Yin, Chen, and Li (2007).

4.5. Backward vehicle simulation models

Backward simulation is the inverse process of the general forward simulation, switching the cause and effect of the forward simulation. In vehicular simulations, when the forward simulation compute the vehicle response corresponding to the driver inputs, backward simulation comprehends the driving torque and energy requirements corresponding to a particular velocity profile input.

Backward simulation finds immense application while realizing vehicle design, which facilitates realization of optimal component sizing in an effective yet simpler manner. Backward facing vehicle models, with scalable models representing vehicle components are often used for this purpose. When modeling scalable components, the energy storage devices and energy converting devices are of prime importance. Energy storage devices such as batteries and fuel cells can be scaled easily, as they are modeled as single cells which can be multiplied as required. Whereas, detailed modeling of energy converts like engine or electric motor is required for successful implementation of backward simulation. Scalable models of IC engine and electric motor with details of energy transformers are explained in detail in Rizzoni, Guzzella, and Baumann (1999).

Unlike the forward simulation models, the backward simulation does not require a driver model; but uses the drive cycles to define the velocity input. Based on the velocity profile, the dynamic forces on the system are calculated and corresponding torque and angular velocity are given to the traction motor/engine. The backward models are assumed to be able to meet the demands of the velocity profile. The models are formulated with the efficiency maps obtained through steady state component testings as well as torque–speed characteristics. This simplifies the calculations, as it reduces to look up tables rather than state equation solution, and improves the efficiency and speed of simulation (Mohan, Assadian, & Longo, 2013). However, the presence of quasi static nature of the backward models degrades the performance with dynamic effects and also makes its difficult to use with HILS. Backward simulation finds great acceptance in energy management strategies (Hofman, Steinbuch, van Druten, & Serrarens, 2006) and several combined design attempts combining forward and backward simulation possibilities are also discussed in literature (Dixon, Stobart, & Steffen, 2015).

5. Transmission model

The maximum tractive effort of the vehicle depends on the actual tractive effort that the highest power plant torque can generate with the available drive-line gear ratios. Thus good knowledge of vehicle power plant and the transmission characteristics may come handy in design of traction controllers. In EV, by suitable selection of traction motor that closely match the desired mechanical characteristics of the EV, the use of complex transmission can be abstained. However, for facilitating motor sizing considering various design constraints, proper transmission gears can be introduced. This Section explains the basic model that can be used to represent the general vehicle transmission model, which can equally be applied for EV modeling.

A schematic representation of an automotive power train is shown in Fig. 7. The major components are: the power plant, clutch or torque converter, transmission, final drive and differential connecting wheels to the drive shaft. Use of the clutch is to couple or decouple the gearbox from the power source in manual transmission whereas torque converter, a hydrodynamic device, is the alternative used with automatic transmission. Function of transmission or gearbox is to supply some gear ratios from input shaft to output shaft to match the speed–torque profile of the source with the load demand. The final drive provides additional speed reduction and the differential facilitates the torque distribution to each wheel.

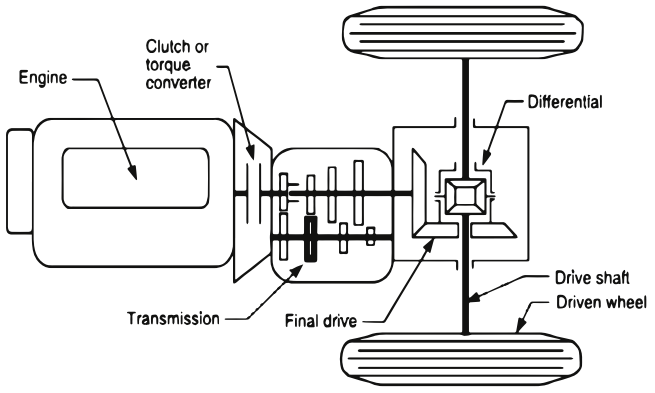

Fig. 7. Schematic diagram of vehicle power train components (Ehsani, 2013).

The torque transmitted T_w from the power source acting on the driven wheels can be represented in terms of T_p, the power source torque output as in (28).

$$T_w = i_g i_0 \eta_t T_p \tag{28}$$

Here η_t represents the drive-line efficiency and i_g, i_0 the gear ratio of the transmission and final drive. i_g can be expressed in terms of input (N_{in}) and output rotating speed (N_{out}) as : $i_g = N_{in}/N_{out}$

The vehicle performance measures can thus be expressed in terms of the gear ratios and dynamic radius r_{dy} as shown in (29)–(31), where (29) represents the effective tractive effort on the driven wheels, (30) gives the wheel rotation speed and (31) represents the translation wheel speed (vehicle speed).

$$F_t = \frac{T_w}{r_{dy}} = \frac{i_g i_0 \eta_t T_p}{r_{dy}} \tag{29}$$

$$N_w = \frac{N_p}{i_g i_0} \tag{30}$$

$$V = \frac{\pi N_w r_{dy}}{30} \text{ m/s} = \frac{\pi N_p r_{dy}}{30 i_g i_0} \text{ m/s} \tag{31}$$

One of the major limiting agent for the peak tractive effort is the force provided by energy source torque with given drive-line gear ratios. This calls for a decorous model of power plant and transmission characteristics for anticipating the overall vehicle performance.

6. Wheel dynamic model

For studies involving critical handling maneuvers, accurate modeling of the various suspension components in the wheel of the vehicle is of high significance. A single DOF simple mass–spring–damper model of the wheels along with the suspension mass is given in Jaiswal et al. (2007). The tires are modeled as a linear spring–damper systems that join the unsprung masses with the road (Jaiswal et al., 2007). On the top, the unsprung masses connect with the body of the vehicle through springs and dampers as shown in schematic diagram given in Fig. 8.

The suspension forces F_{suspi}, corresponding to the motion of unsprung masses relative to the vehicle body are :

$$\begin{aligned}
F_{susp1} &= -K_f[(z - t_{rf}\phi - a\theta) - z_{wheel1}] - C_f[(z' - t_{rf}p - aq) - z'_{wheel1}] \\
F_{susp2} &= -K_f[(z - t_{rf}\phi + a\theta) - z_{wheel2}] - C_f[(z' + t_{rf}p - aq) - z'_{wheel2}] \\
F_{susp3} &= -K_f[(z - t_{rf}\phi - a\theta) - z_{wheel1}] - C_f[(z' - t_{rr}p - aq) - z'_{wheel3}] \\
F_{susp4} &= -K_f[(z - t_{rf}\phi + a\theta) - z_{wheel2}] - C_f[(z' + t_{rr}p - aq) - z'_{wheel4}]
\end{aligned} \tag{32}$$

p, q represents roll and pitch differentials, z, z_{wheeli} vertical displacements of vehicle and the four wheels. K_f, C_f wheel-rate and damping functions, t_{rf}, t_{rr}, the half-tracks and a, b are distance of frame origin from the front and rear axles. Considering, the rigid suspension reactions and anti-roll bar effects with the aforementioned suspension force expressions, the dynamic equations of the unsprung masses for the vertical movement can be obtained as:

$$\begin{aligned}
&- F_{susp1} - [K_{tire} \cdot z_{wheel1} + C_{tire} \cdot z'_{wheel1}] + M_{wheel1} \cdot g \\
&\quad - M_{wheel1} \cdot z''_{wheel1} - \frac{K_{roll}(\phi + \phi_{wheel1})}{2.t_{rf}} - F_{zy1} - F_{zx1} = 0 \\
&- F_{susp2} - [K_{tire} \cdot z_{wheel2} - C_{tire} \cdot z'_{wheel2}] + M_{wheel2} \cdot g \\
&\quad - M_{wheel2} \cdot z''_{wheel2} + \frac{K_{roll}(\phi + \phi_{wheel2})}{2.t_{rf}} - F_{zy2} - F_{zx2} = 0 \\
&- F_{susp3} - [K_{tire} \cdot z_{wheel3} + C_{tire} \cdot z'_{wheel3}] + M_{wheel3} \cdot g \\
&\quad - M_{wheel3} \cdot z''_{wheel3} - \frac{K_{roll}(\phi + \phi_{wheel3})}{2.t_{rf}} - F_{zy3} - F_{zx3} = 0 \\
&- F_{susp4} - [K_{tire} \cdot z_{wheel4} - C_{tire} \cdot z'_{wheel4}] + M_{wheel4} \cdot g \\
&\quad - M_{wheel4} \cdot z''_{wheel4} + \frac{K_{roll}(\phi + \phi_{wheel4})}{2.t_{rf}} - F_{zy4} - F_{zx4} = 0
\end{aligned}$$

An additional term $\phi_{wheel1-4}$ is appended to the roll angle of body, ϕ so as to make up for the anti-roll bar force generated due to unequal wheel vertical displacement, when on undulated surfaces. This added roll angle, can be calculated using (33)–(34) based on simple geometrical considerations.

$$\phi_{wheelf} = atan\frac{z_{wheel1} - z_{wheel2}}{2.t_{rf}} \tag{33}$$

$$\phi_{wheelr} = atan\frac{z_{wheel3} - z_{wheel4}}{2.t_{rf}} \tag{34}$$

The inclusion of these terms accounts for all phenomena like anti-roll, anti-dive and jacking and is a better option to other treatments like roll-center approach used often.

The wheel model discussed is equally applicable for application in formulating the general vehicle dynamic model as well as for the EV modeling.

7. Tire modeling

An apposite tire model, depicting the tire longitudinal and lateral flexibility is of great importance while formulating the EV model for complex maneuvering control applications, particularly in the design of ABS for EV. This Section discusses various tire models which are used for EV modeling and are equally applicable for any vehicle. On the basic level, the tire modeling process utilizes the measured tire data in conjunction with the interpolation method for representing tire force characteristics. Most of the tire models used currently in simulation analysis of vehicle use empirical formulation of the measured tire data (Hegazy et al., 1999). As a result of the interaction with road, six components of forces and associated moments are generated in tire. The components are (i) vertical tire force, (ii) lateral force, (iii) longitudinal traction force, (iv) self orienting moment, (v) overturning moment (vi) rolling resistance moment. A good model incorporates the dynamic representation of all these forces.

One of the most renowned tire model in vehicle dynamics study is the 'Magic Formula' tire model, which was developed by Bakker et al. (1989). This is a simple model but can be precisely calculated from basic parameters, the longitudinal as well as lateral tire forces. Followed by the magic formula, a synopsis of the three main transient tire models — stretched string, modified stretched-string and contact mass transient model along with a piece wise-linear tire model is given. The influence of transient tire characteristics in vehicle handling problems, particularly in those involving ABS has been discussed in Jaiswal, Mavros, Rahnejat, and King (2009).

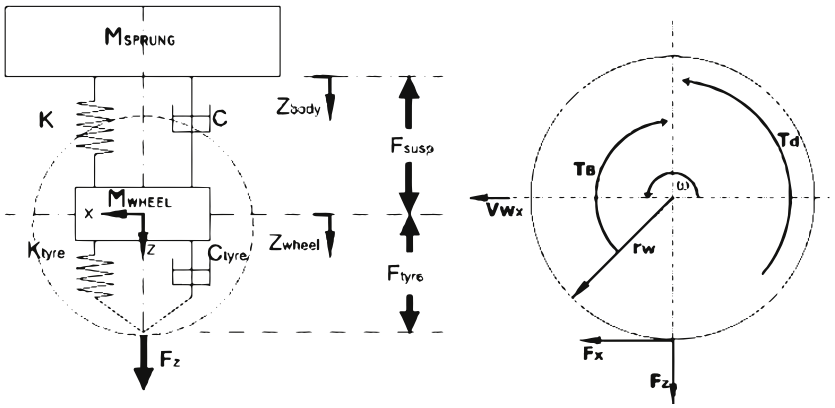

Fig. 8. Free body diagram of suspension and wheel (Jaiswal et al., 2007).

7.1. The magic formula

The Magic formula (MF) was formulated by Bakker, Pacejka, and Lidner in 1989 (Bakker et al., 1989), after conducting a series of tire measurements in stationary conditions on the road. The resulting data was represented using mathematical equations on the basis of a formula. The MF can be used to obtain all characteristics of self aligning torque, side force, and brake force with great accuracy. The basic magic formula can be represented as in (35).

$$y = Dsin[C \cdot tan^{-1} B - E(B - tan^{-1} B)]$$
$$Y(x) = y(x) + S_V$$
$$x = X + S_H \tag{35}$$

Here X depicts the elementary input variable — the side-slip or longitudinal slip, and Y depicts the elementary output variable — lateral/longitudinal force or self-aligning torque. The coefficients B, C, D, and E in the MF correspond to some of the describing measures of the tire that depends on the normal load, F_z, the camber angle, γ, and a number of secondary constants, similar to the S_H and S_V parameters.

Using the magic formula a compact empirical tire model can be obtained which can accurately represent the tire behavior even during the events of combined cornering and braking.

7.2. Stretched string model

A singular order differential equation is used to incorporate the tire transient behavior, representing the first-order relaxation length defined as the compliance of carcass with regard to the wheel in x and y directions. The method was originally formulated to analyze the tire shimmy motion (Kuiper & Oosten, 2007). The string model when considered in its simple form, confine to a uni-contact-point tire model. The adjoin patch and the wheel surface are connected through lateral and longitudinal spring, which represents the carcass stiffness in respective directions. Consecutively, the contact patch can slide relating to the surface in x and y directions. A schematic representation of the model as represented by Pacejka is shown in Fig. 9, where a stretched-string suspended to the rim is used to model the tire belt.

The dynamics of the lateral deflection (v_1) and longitudinal deflection (u_1) of the contact point with respect to the rim can be articulated as follows :

$$\sigma_\alpha \frac{dv_1}{dt} + |U_w| v_1 = \sigma_\alpha V_{sy} \tag{36}$$
$$\sigma_k \frac{du_1}{dt} + |U_w| u_1 = -\sigma_k V_{sx} \tag{37}$$

The relaxation lengths (σ_k, σ_α) can be expressed as a function of vertical load. Now, for calculation of forces and moment, the magic formula can be used considering the transient values of slip and slip angle found as in (38) and (39).

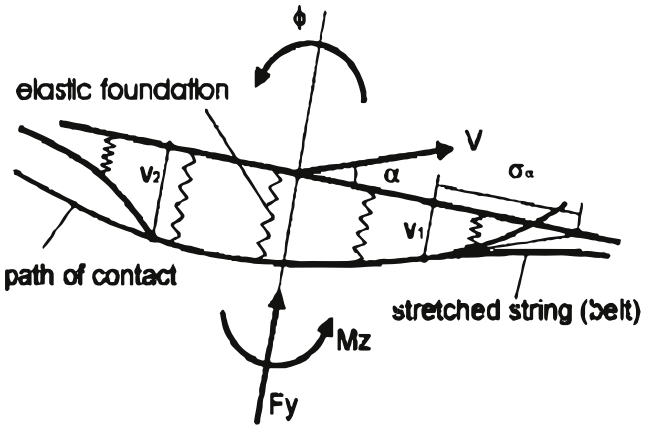

Fig. 9. Stretched string tire model top view (Kuiper & Oosten, 2007).

$$k' = \frac{u_1}{\sigma_k} sign(U_w) \tag{38}$$
$$\alpha' = atan(\frac{v_1}{\sigma_\alpha}) \tag{39}$$

7.3. Modified stretched-string model

The simple stretched string model does not consider tire slip into account and the relaxation length is realized as a function of vertical load. This assumption neglects the change in the relaxation length with an increasing slip angle which is the case in practice. In order to surmount this issue of the basic string model, (Pacejka, 2012) put forward a modified version of stretched-string model including an elastic tire tread element.

The first-order relaxation length equations in the modified one are alike the basic model except that the lengths σ_α and σ_k are substituted with σ_α^* and σ_k^* respectively, which are obtained, taking into account the vertical load and slip variation transient effects as in (40) and (41).

$$\sigma_\alpha^* = \frac{1}{C_{F_y}} \frac{F_y}{tan\alpha'} = \frac{\sigma_{\alpha 0}}{C_{F\alpha}} \frac{F_y}{tan\alpha'} \simeq \frac{\sigma_{\alpha 0}}{C_{F\alpha}} \frac{|F_y'| + C_{F\alpha}\epsilon_F}{|tan\alpha_f'| + \epsilon_F} \tag{40}$$

$$\sigma_k^* = \frac{1}{C_{Fx}} \frac{F_x}{k'} = \frac{\sigma_{k0}}{C_{Fk}} \frac{F_x}{k'} \simeq \frac{\sigma_{k0}}{C_{Fk}} \frac{|F_x'| + C_{Fk}\epsilon_F}{|k'| + \epsilon_F} \tag{41}$$

$\sigma_{\alpha 0}$ and σ_{k0} represents the relaxation length at $\alpha = 0$ and $k = 0$ respectively, which can be obtained as:

$$\sigma_{\alpha 0} = \frac{C_{F\alpha}}{C_{F_y}} \qquad \sigma_{k0} = \frac{C_{Fk}}{C_{Fx}}$$

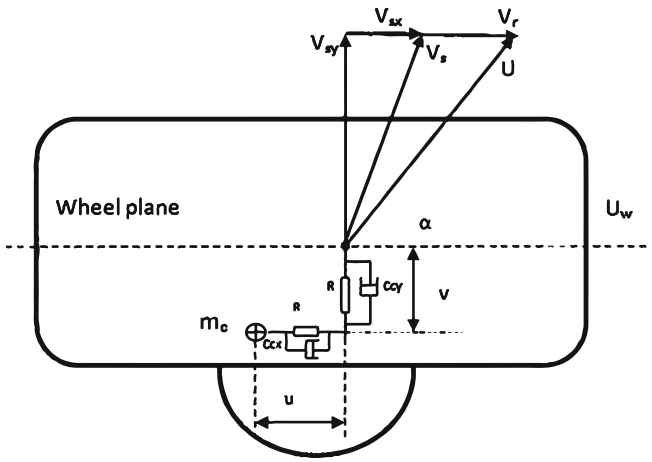

Fig. 10. Contact mass tire model.

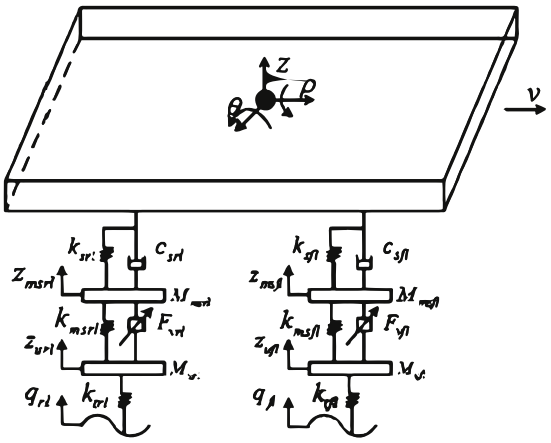

Fig. 11. In-Wheel motor dynamic model (yang Wang & ning Yang, 2017).

Using similar procedure followed in the basic model, the force and moment equations can be computed with the help of magic formula.

7.4. Contact mass transient model

The stretched-string models follow the relaxation length concept, that incorporates a delay in the reaction to lateral slip or longitudinal slip due to consideration of carcass abidance and contact slip attributes. This lag depends on the vertical load as well as wheel slip changes; thus reducing the relaxation length at elevated levels of slip. Nonetheless, this method is mathematically very unstable and can become somewhat cumbersome in combined slip the situations. As a solution, a faintly different approach can be used, where carcass springs are explicitly incorporated into the model for the separation of the carcass abidance and contact slip attributes Pacejka (2012). As shown in the Fig. 10, the contact area is now characterized with inertia facilitating its deflection in the peripheral as well as lateral domains corresponding to the rim. Thus the carcass compliance along with contact patch slip model by design handle the lag due to the vertical load, thereby decreasing the lag with an increase in slip.

This model was first used by Pacejka and Besselink (1996), and was included in their magic formula transient tire model version 1997, which later got included in the PAC 2002 tire model.

In order to enable faster computations, a simple relaxation length model is also incorporated in the contact mass model as given in (42) and (43).

$$\sigma_c \frac{\mathrm{d}\alpha'}{\mathrm{d}t} + |V_w| \alpha' = -V_{sy}^* \tag{42}$$

$$\sigma_c \frac{\mathrm{d}k'}{\mathrm{d}t} + |U_w| k' = -V_{sx}^* \tag{43}$$

The longitudinal and lateral deflection rates can be found using the slip speed differences. The forces acting on the wheel rim can then be calculated after obtaining the longitudinal and lateral deflections.

7.5. Piece-wise linear tire model

Even when the MF approach yields a more realistic tire behavior, it is a complex method requiring many experimental coefficients. A piece wise linearization method is discussed in Liu et al. (2013), which uses fewer coefficients. This is under the condition that the longitudinal as well as lateral tire forces are linear, for smaller slip angle or the slip ratio. Most of the typical driving is usually done in this linear region. The tire shows nonlinear behavior with a gain in the slip angle/slip ratio. Thus a piece wise function can be utilized to describe the tire model.

8. In- wheel modeling

While talking about the tire modeling of electric vehicles, it is interesting to discuss about the INW concept used exclusively for EV applications. The popularity of INW in EV applications is due to structured configuration, less weight, highly effective transfer of power and accurate speed and torque control. However, issues created due to the decentralized INW structure cannot be neglected. Vigorous research is going on in this aspect, where for the proper analysis and solution, a detailed understanding of the motor parameters and their effects on vehicle dynamics is needed.

The permanent magnet BLDC motors, because of their increased power density efficiency become the prime option in INW. They are shadowed by the cost of magnets as well as the reduction in flux density during high operating temperature reducing the torque capacity of the machine (Wang & Fahimi, 2012). Recent studies clearly state the prominence of SRM over other motors for EV applications due to simpler control, increased efficiency, constant power at high speed, and robust artifact (Naayagi & Kamaraj, 2005). In the following Section, a non linear dynamic model of INW with SRM stator is presented.

8.1. In-wheel motor EV model

For the purpose of simulating the In-wheel motor EV dynamic responses, a In-wheel model is developed in yang Wang and ning Yang (2017) using the Fig. 11, including Switched Reluctance Motor stator, rotor and vertical forces in the EV.

The body vibration as well as roll motion dynamics are considered for vehicle dynamics. The set of Eqs. (44) represents the upright movement of the tire total mass, rims and the motor rotors corresponding to each corner with reference to Fig. 11.

$$\begin{aligned}
M_{ufl}\ddot{z}_{ufl} &= k_{mfl}(z_{mfl} - z_{ufl}) - k_{tfl}(z_{ufl} - q_{fl}) + F_{vfl} \\
M_{ufr}\ddot{z}_{ufr} &= k_{mfr}(z_{mfr} - z_{ufr}) - k_{tfr}(z_{ufr} - q_{fr}) + F_{vfr} \\
M_{url}\ddot{z}_{url} &= k_{mrl}(z_{mrl} - z_{url}) - k_{trl}(z_{url} - q_{rl}) + F_{vrl} \\
M_{urr}\ddot{z}_{urr} &= k_{mrr}(z_{mrr} - z_{urr}) - k_{trr}(z_{urr} - q_{rr}) + F_{vrr}.
\end{aligned} \tag{44}$$

The vertical force F_v exerted on the mass of tire, hub, housing and SRM, will affect the SRM air gap deflection, which can further affect vehicle performance. The air gap deflection can be obtained from SRM stator and rotor vertical relative movement. A detailed SRM vertical force model is also presented in yang Wang and ning Yang (2017) which will be useful in predicting the vertical force, obtained from the torque on the wheel.

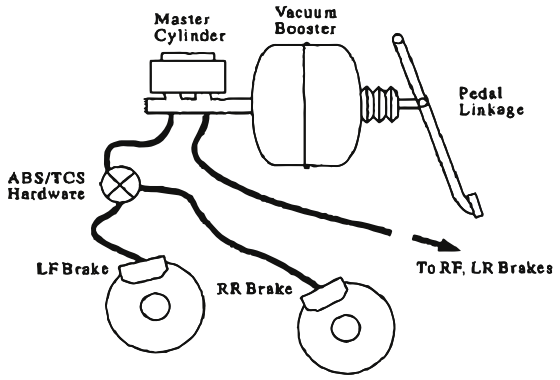

Fig. 12. Components of the brake system (Gerdes & Hedrick, 1999).

9. Brake system models

While formulating EV models for design purpose, it is seen that the modeling of the brake is often neglected, yet it is of high importance in specific applications like the kind of ABS. In this Section models of hydraulic brakes along with modeling of electro-mechanical braking used in electric vehicles will be discussed.

9.1. Hydraulic brake system modeling

Hydraulic brake systems, used in conventional vehicles transmits the braking force applied on the brake pedal by means of fluid pressure to the wheels. The disk brake system along with other major parts of the hydraulic brake system are shown in Fig. 12. The vacuum booster is used to create a simple and robust amplification of the force on the brake pedal, which is done by utilizing the pressure difference that exists in engine intake manifold with respect to the atmosphere. Detailed discussions of the complex vacuum booster model with details on different components of the brake are given in Gerdes and Hedrick (1999). The brake hydraulics system plays three major roles during braking. Firstly, they serves as apt interface between the driver input and the brake system, thus facilitating force carry-over with amplification. Secondly, the multiple circuit design acts as a reliable safety function with back up in case of a failure in one circuit. Ultimately, during rapid deceleration, they are able to realize hydraulics proportion braking by the reduction of the rear wheels relative brake force. The brake hydraulic system can be represented as shown in Fig. 13(a). A brake hydraulics four-state model with an overview of operation of the hydraulic system are given in detail in Gerdes and Hedrick (1999).

9.1.1. Reduced brake models

In relatively less complex design cases where ABS or proportioning come into play, variations across wheels are not of much importance as compared to the net amount of braking produced. For such applications the four state model will be unnecessary and may exhibit surplus complexity for process including controller design or simulation of an entire vehicle. A reduced model from the four state model can be obtained by the inclusion of only a few hydraulic states.

Two state reduced brake model

The two state model is formulated by considering only pressure change in individual circuit and neglecting the individual wheels behavior. The hydraulic model can be reduced as shown in Fig. 13(b). where the two states are the fluid volumes displaced into the primary circuit (V_p) and secondary circuits (V_s).

From the Fig. 13(b), the displacements, x_{mcp} and x_{mcs} can be obtained using area of the master cylinder (A_{mc}) as in (45).

$$x_{mcs} = \frac{V_s}{A_{mc}} \qquad x_{mcp} = \frac{V_p}{A_{mc}} + x_{mcs} \tag{45}$$

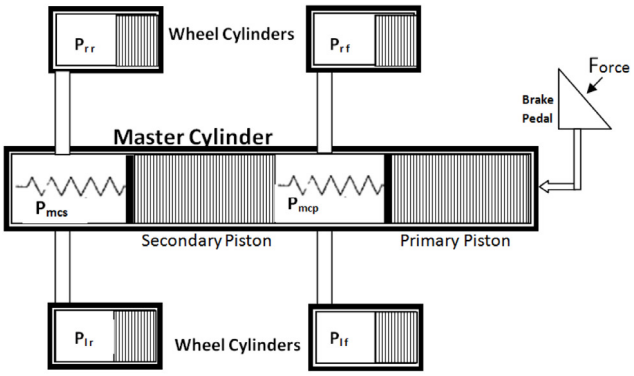

(a) Schematic of Brake hydraulic system.

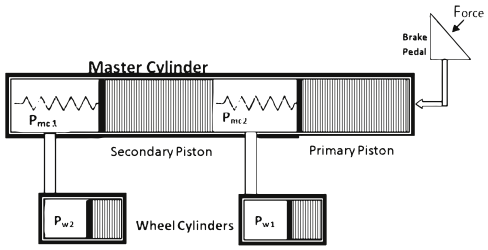

(b) Reduced dual circuit model.

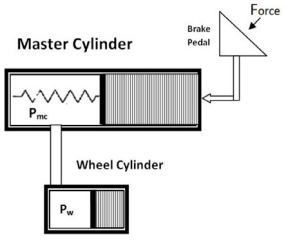

(c) Reduced single circuit model.

Fig. 13. Hydraulic Brake Models.

The two state equations for the system corresponding to the V_p and $V_s$can be formulated as shown in (46) and (47).

$$\dot{V}_p = \sigma_p C_{qp} \sqrt{(|P_{mcp} - P_{wp}|)} \tag{46}$$

$$\dot{V}_s = \sigma_s C_{qs} \sqrt{(|P_{mcs} - P_{ws}|)} \tag{47}$$

where P_i represents the fluid capacity and C_{qi} is flow coefficient of ith element. The brake torque can be thus be analogously found for each circuit in terms of the brake gain and push out pressure.

Single state reduced brake model

A further simplified model can be obtained in cases where, it is not important to consider the two hydraulic circuits are not important. The simplification can be done by modeling the hydraulics as shown in Fig. 13(c), as a single equivalent brake linked to the master cylinder. The model can be obtained as similar to the primary circuit equations corresponding to the two state models (Gerdes & Hedrick, 1999).

9.2. Regenerative braking

Regenerative braking system employed in the EVs contribute highly in improving the energy efficiency of the vehicle. The system converts the kinetic energy released during braking into electrical energy that is used to recharge the battery. The system constitutes of electric motor/generator with the power converters which are closely controlled

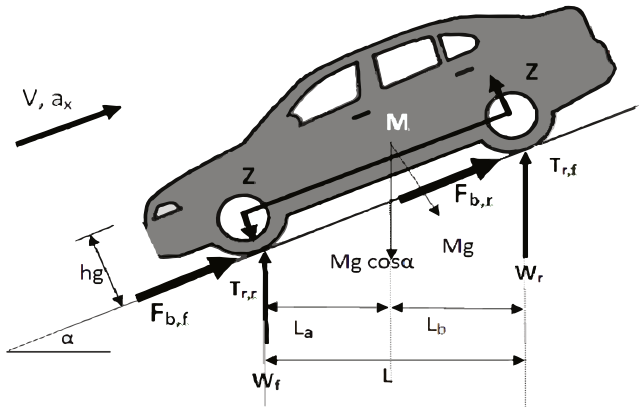

Fig. 14. Dynamic vehicle model during braking.

by the central control unit. Since the safety and driving comfort greatly depends on the braking, especially on fallible road conditions, superior electrical braking control methods are necessary. For design and formulation of the control techniques, dynamic models of the braking force and the load acting on the vehicle are of great significance.

A detailed dynamic model during braking is given in Mutoh, Hayano, Yahagi, and Takita (2007), that can be used in braking control design. The model can be stated with reference to Fig. 14. The braking force F_b acting to push back the wheel touching the ground and the forward inertial force of center of gravity F_I are used to find the individual wheel braking torques. The vehicle deceleration sensed using a sensor is used to calculate the braking force as:

$$F_b = M.(a_x) = M.-(\frac{dV}{dt}) \tag{48}$$

When running on graded roads, the deceleration measured by the onboard sensor will be the resultant of the deceleration on plain roads and acceleration due to gravity, g.sinα, where α is the road angle.

The individual braking forces of front and rear wheels can then be found in terms of the vehicle load movement z, and vehicle dimensions as in (49).

$$\begin{aligned} F_f &= \mu \cdot (W_f + z) = \mu \cdot (W_f + |\ \frac{F_b \cdot h_g}{L}\ |) \\ F_r &= \mu \cdot (W_r - z) = \mu \cdot (W_r - |\ \frac{F_b \cdot h_g}{L}\ |) \end{aligned} \tag{49}$$

As the braking forces are functions of the friction coefficient, the force distribution is done based on the distribution ratios, R_f and R_r. The wheel braking torque references for the controller can be formulated using R_f, R_r and the total braking reference torque, τ_b^* obtained from brake pedal (Mutoh et al., 2007). The mass of the vehicle changes with loading, accurate estimation of the mass will be required.

Electro-mechanical Brake systems were introduced to improve the safety and energy efficiency of the vehicles. It replaces the hydraulic brake components with electronics, thereby simplifying the brake system. Even though it increases the flexibility of the system, specific control strategies are to be designed. A detailed electro-mechanical brake system model and intelligent control is given in Hwang, Kim, Kim, and Jung (2010). Regenerative Braking along with hydraulic braking systems existing in vehicles calls for Cooperative Control systems, which control the share of the braking force required between the braking systems (Ko et al., 2013, 2015). A novel regenerative braking control strategy for optimal braking torque distribution between electrical and frictional braking is discussed in Xu, Chen, Zhao, and Ren (2019), which maximizes the safety as well as energy recovery efficiency.

Table 1
Comparison of battery models.

Battery model	Remarks	Features
Shepherd model	Simplest electrochemical model	Battery behavior modeled in terms of voltage and current
Unnewehr model	Simplified shepherd model	Variation in resistance modeled in terms of SOC
Nernst model	Modified Shepherd model	SOC modeled as exponential function
Combined model	Most accurate electro chemical model	Combination of the three electrochemical models
Rint model	Equivalent circuit battery model	Simplest considering only internal resistance
Thevinin model	Based on Rint model	RC circuit added in series to consider polarization
Dual polarization model	Modified Thevenin model most accurate model	Two RC circuits to consider concentration and electro-chemical polarization separately

10. Battery models

In the simulation study and analysis or design of control strategies for EVs, an accurate model of the battery behavior is of high importance. They are particularly of high interest for accurate battery state estimation in the model-based battery management system. The basic six battery models has been described briefly in Chan (2000) with focus of the most simple model among them which can accurately represent most of the important features of the EV batteries. In a more recent work (He, Xiong, Guo, & Li, 2012), the model equations and comparison of seven modern battery models- (i) Shepherd model, (ii) Unnewehr Universal model, (iii) Nernst model, (iv) Combined model (Plett, 2004), (v) Rint model (Chan, 2000) (vi) Thevenin model (Salameh et al., 1992), and (vii) Dual polarization (DP) model (He, Xiong, Zhang, Sun, & Fan, 2011), with an evaluation procedure for the battery models through experimentation is available. The characteristics of the above mentioned battery representative models are summarized in the Table 1.

Based on the several experimental tests, it was found that the Thevenin and Dual polarization model exhibits better dynamic performance (Chan, 2000), of which the DP model exhibits better performance as the voltage relaxation has a more svelte simulation. Also, the formulated battery general equivalent circuit models (GECMs) model with dual RC networks, declared the Dual polarization model as the optimal model for the simulation of Li-ion battery. Therefore, the Dual polarization model is described in the following Section.

10.1. Dual polarization model

Dual polarization (DP) model is basically a modified Thevenin model formulated by considering the polarization characteristics of the Lithium-ion battery (He et al., 2011). Even with the high acceptance of the Thevenin model, it inherits the disadvantage of having inaccuracy due to the possibility of change in elements corresponding to the state of the battery. DP model is formulated from the Thevenin model by introducing an additional RC branch to it as given in Fig. 15.

The DP model consists of three main parts - U_{OC} open circuit voltage, internal resistances and equivalent capacitance. The internal resistance consists of the ohmic resistance (R_o), concentration polarization resistance (R_{pc}) and electro-chemical polarization resistance (R_{pa}). The equivalent capacitance consists of the electro-chemical and concentration polarization capacitance C_{pa} and C_{pc}, which represent the charging/discharging transits transient response. The electrical action of the circuit can be represented as in (50) with reference to Fig. 15.

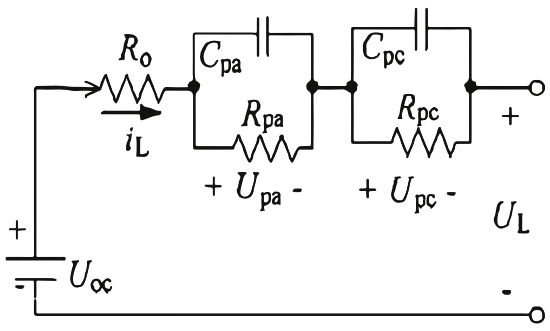

Fig. 15. DP model battery equivalent circuit (He et al., 2011).

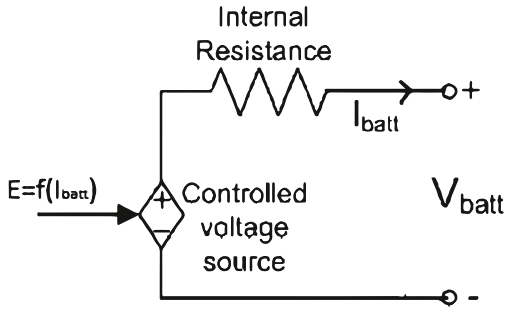

Fig. 16. Nonlinear battery model.

$$\dot{U_{pa}} = \frac{-U_{pa}}{R_{pa}C_{pa}} + \frac{i_L}{C_{pa}}$$
$$\dot{U_{pc}} = \frac{-U_{pc}}{R_{pc}C_{pc}} + \frac{i_L}{C_{pc}}$$
$$U_L = U_{OC} - U_{pa} - U_{pc} - i_L R_O \quad (50)$$

10.2. Non linear battery model

Another 'easy-to-use' battery model which can be used for dynamic simulation software is presented in Ye, Miao, Lei, and Li (2016). This simple model requires only the battery State-Of-Charge (SOC) as a variable thus simplifying the algebraic solution. The model which can precisely characterize four versions of battery chemistry becomes easy to use as the parameters can be identified from the discharge curve provided by the manufacturer using the specified method.

The battery is model is given in the Fig. 16, and the controlled source equation representing it can be written as in (51).

$$E = f(I_{batt}) = E_0 - K\frac{Q}{Q - i_t} + A.exp(-B.\int idt)$$
$$V_{batt} = E - i.R \quad (51)$$

In spite of the simplicity in the model, it has certain limitations. The minimum capacity of the battery is set as 0 V and the maximum capacity is not limited at all. This can lead to a situation with maximum SOC greater than 100 percentage, during the overcharging of the battery.

11. Fuel cell models

One of the most promising alternate source of electrical energy for EV is the Fuel cells (FC), which is gaining increasing acceptance owing to its renewable and environment-friendly nature. FCs are a category of electro-chemical converters where, the fuel chemical energy gets converted into DC electricity. The major difference with the battery is that chemical reactants/fuels must be supplied from external source to a fuel cell, but for a battery, they are inherent.

The fuel cells can be classified based on the type of electrolyte used as shown in Fig. 17. Various fuel cell models with their operating principles are well explained in the diagram (Gao, 2014). Of the different forms of fuel cells available, the Polymer Electrolyte Membrane (PEMFC) and Direct Methanol (DMFC) are the most popular ones in EV owing to their adaptability for application in mobile cars. PEMFC, with its solid electrolyte which will not leak or crack and low operating temperatures was the most popular one. DMFC, which is a relatively recent addition to fuel cell technologies, is gaining significant interest in fuel cell powered electric vehicle domain. In the following Sections, the general models of PEMFC and DMFC will be discussed.

11.1. PEMFC modeling

A PEMFC consists of the platinum coated anode and cathode sandwiching a proton exchange membrane. The platinum acts as the catalyst, which accelerates the ionization of H_2 gas which is given to the anode as H_2 ions(+ve) and electron(−ve). The proton exchange membrane allows only the positively charged H_2 ions to move to the cathode blocking electrons, which produce a current (Zaidy, Pokharkar, Krishnan, & Sonawane, 2014).

The dynamic model of the PEMFC considers the output voltage variations with respect to alterations in the FC current, thus including the load variation effects. A single fuel cell output voltage can be expressed as the resultant of the thermodynamic potential (E_N), Ohmic (V_{oh}) and Activation (V_{act}) Voltage loss as follows:

$$V_{FC} = E_N - V_{act} - V_{oh} - V_{con} \quad (52)$$

To increase the fuel output, usually individual PEMFC cells are combined to form a PEMFC stack. The individual expressions for the electrochemical models of voltage losses are elaborated in Xu and Xiao (2011).

11.2. DMFC modeling

Although PEMFC acts as the favorite FC for automobile applications, there is a demand for a better FC which does not require a reformer and without the storage and safety concerns raised by the hydrogen storage. Direct Methanol Fuel Cells (DMFC) have emerged as an alternative to PEMFC.

Several DMFC models are available in literature which can be grouped as analytical, semi-empirical, and mechanistic models. Detailed description of various types of models along with a comparison is given in Pofahl (2012). Analytical modeling gives a better perceptive on the impact of basic parameter on the FC performance, which require accurate knowledge of the variation in cell voltage with current density. A variety of analytical models can be found in the literature (Guo & fang Ma, 2004; Kulikovsky, 2002) which can be selected based on the dynamics required. Semi-empirical models for DMFC are also available in abundance in literature (Argyropoulos, 2003; Chiu, Yu, & Chung, 2011; Sundmacher et al., 2001; Wang, Zheng, Au, & Plichta, 2008). Semi-empirical models are utilized to assess the FC performance with respect to operating conditions like pressure, temperature and heat using empirical models (Chiu, 2010; Dohle & Wippermann, 2004). These models require less computational effort as they use basic algebraic equations. The mechanistic models are transport models describing heat, momentum, mass transport and similar fundamental phenomenon (Ko, Chippar, & Ju, 2010; Zou, He, Miao, & Li, 2010). However, they are more complex than other types of models as they require differential and algebraic equations (Basri & Kamarudin, 2011; Delavar, Farhadi, & Sedighi, 2010). Nevertheless, mechanistic model are able to explain the fundamental phenomena occurring in the fuel cell in detail.

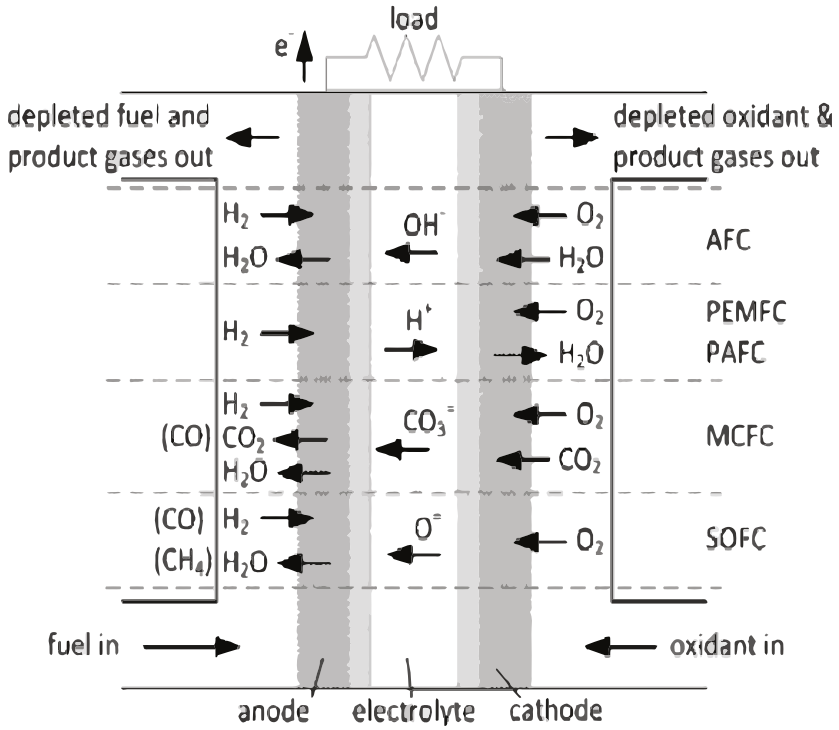

Fig. 17. Types of fuel cell with electrochemical reactions (Gao, 2014).

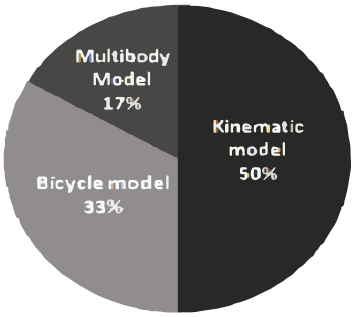

Fig. 18. Statistics of the type of vehicle dynamic model used in control design for EV.

12. Discussion and conclusions

The paper embodies a survey of various available EV models with emphasis on its control applications. The paper will act as a guide for the inquisitive researchers in the domain of EV control. Starting with the fundamental dynamic model of the vehicle, derived from the physics of motion, a variety of dynamic models of the vehicle are presented. More complex multi-body models, formulated by considering the suspension geometry of the vehicle, will be well suited in applications involving critical maneuvering and handling stability analysis. A simpler bicycle model of the vehicle with reduced DOF is also presented, which is optimal for less critical control requirements. The percentage of usage of each model in various control design projects can be summarized as shown in Fig. 18.

Following the study of various control designs realized in EV, it was found that for the realization of each design, certain major dynamic variables are crucial as compared to others. Thus, for the successful design and realization of a control aspect, a proper definition of the concerned variable in the vehicle model is crucial. While selecting a model for the analysis and control design, it should be made sure that the selected model can properly define the variables of interest. Table 2 summarizes various control domains active in the EV applications along with the variables of interest corresponding to each of them.

Table 2
Variables of interest in control domains.

Control	Variables of interest
Longitudinal motion control	Power train output torque, Velocity profile
Lateral motion control	Yaw rate, Cornering Speed
Combined longitudinal and lateral control	Torque, yaw and cornering dynamics, velocity profile
Traction control	Traction force dynamics based on load interaction, wheel dynamics
Steering control	Steering kinematics
Trajectory following control	Slip angle, Yaw rate, Trajectory dynamics
Range Extension Control	Tire slide slip angle, Load transfer model, Force distribution model
Yaw Stability Control	Yaw model, differential moment dynamics between wheels
Cornering stability control	Slip ratio, yaw rate, wheel torque
Wheel slip control	Tire Slip, Driving and Braking Slip
Handling stability control	Vehicle speed, Yaw rate, Slide slip angle
Energy management	Power plant dynamics, SOC dynamics

Besides, for the design of several critical control requirements, accurate description of the characteristics of the different physical components of the vehicle is obligatory. Finding the accurate models of these components is of paramount importance without which it may yield a less optimal model. The paper summarizes various models available for each of the physical components in the vehicle, making it is easier for the selection of an optimal model for the designer. The mathematical model of the vehicle power plant and transmission characteristics has been presented in depth.

One of the major components which contributes highly on vehicle control is the wheel and tire dynamics of the vehicle. Unfortunately, it was found that many control designs have neglected the tire dynamics as well as the wheel suspension dynamics. A variety of tire models

are presented in the paper, ranging from simple, linear dynamics to complete, transient characteristics. One of the most used forms of tire models is the basic magic formula, which when supplemented with the more detailed stretched-string models can give a very absolved picture of the tire dynamics. The transient tire models will be well suited for ABS as well as cornering stability control aspects, whereas for simpler requirements linear models will be sufficient.

One of the most neglected dynamics of the vehicle is those of the brake and associated systems. Rarely are these models used in association with the vehicle dynamics for analysis and control design. This can lead to failure or unexpected results while implementing the designed control strategy in a real-time vehicle. Simplified, reduced-order models are presented in the paper, which will encourage the use of these dynamics while designing. Using these guidelines, a suitable brake model can be considered for a more accurate and reliable design of control. As other component models can be adopted from conventional vehicles, the battery models are more specific for EV. A detailed comparison of the various battery models mentioning their dynamics equations is made. Also, the most accurate DP model is described in detail along with a more latest non-linear battery model. Discussions are mainly confined to the EV domain, which can very well be extended to the hybrid domains with appropriate supplements. To facilitate the applications in hybrid as well as Range Extended EV, the modeling of fuel cell energy source has been included.

12.1. Identified gaps in literature

- Standard numerical models representing power consumption and mechanical performance of the vehicle needs to be derived for designing model-based solutions for improving the energy efficiency of the vehicle.
- Vehicular position-dependent models are not available, most of the available models are time-based.
- Accurate representation of the cross-coupling dynamics that exists between various electrical, as well as mechanical components of the vehicle, needs to be formulated.
- Numerical models facilitating the application of state of the art control techniques based on artificial intelligence can accelerate the research on EV domain.

12.2. General framework for EV modeling

Modeling of the EV begins with accurate details of the sizing of the power train. EV component sizing can be realized by using the kinematic model of EV given in Section 3.2, which helps in finalizing the component sizing as per vehicle requirements. To initiate controller design to reach desired performance specifications, select a suitable vehicle dynamic model with suitable complexity so as to address the desired controllability of the system. Table 2 can be used for the same, which provides suitable vehicle models that include variables of interest corresponding to each control requirement. The general vehicle dynamics can be supplemented with accurate mathematical representations of each physical components to formulate a more realistic EV model. Suitable models for representing the transmission based on the gear ratio requirements can facilitate accurate mechanical modeling of the EV. One of the major, yet neglected part in modeling is the wheel, tire–ground dynamics of the vehicle. Accurate modeling of this can be achieved by utilizing any of the models represented in Sections 6 and 7. The selection is done based on the complexity of the tire dynamics required in the control realization. Following the tire dynamics, a proper brake system modeling is to be included in the EV model. Neglecting this can result in unexpected behavior of the designed controller under critical steering conditions.

All the preceding steps are in general applicable for any vehicle modeling, however specifically for EV modeling, accurate representation of the electrical behavior of the battery source is important. Of the various electrochemical and equivalent circuit models given in Section 10, a suitable model of desired complexity can be chosen. Auxillary energy sources to append battery sources for improving the driving range of the vehicle is a modern practice. Fuel cell models which can act as such an auxiliary source can be included for range-extended EV modeling. Regenerative braking system modeling is of prime importance while modeling EV for ABS and TC control realizations which can be facilitated by Section 9.2.

Backward simulation models can be used to obtain the energy consumption model and to verify the sizing calculations concerning the requirements.

12.3. Our contributions

The paper, first of its kind, can usher the enthusiastic researchers working on control design for electric vehicle applications. A range of vehicular dynamic models is presented, varying in complexity, which can be used to select a suitable dynamic model for an EV as required by the control demand. The paper compiles various available models for all physical components of the EV namely — transmission, brakes, batteries, and tire dynamics. The control design implementation can be highly facilitated by considering the dynamics of these often neglected components, thus providing a better approximation of the physical dynamics of the vehicle. The considerations can be used in the future to formulate better ABS and Torque control realizations for EV by including wheel and tire dynamics. Paper does a comparative study of models available for various energy sources used in EV power train such as batteries and fuel cells. This can cater support for advanced research in EV energy management problems as well in range extender solutions for driving range extension of EV.

Declaration of competing interest

The authors declare that they have no known competing financial interests or personal relationships that could have appeared to influence the work reported in this paper.

References

Abe, M. (2015). Vehicle body roll and vehicle dynamics. In *Vehicle handling dynamics* (pp. 153–186). Elsevier, http://dx.doi.org/10.1016/b978-0-08-100390-9.00006-3, URL https://doi.org/10.1016%2Fb978-0-08-100390-9.00006-3.

Aligia, D. A., Magallan, G. A., & Angelo, C. H. D. (2018). EV traction control based on nonlinear observers considering longitudinal and lateral tire forces. *IEEE Transactions on Intelligent Transportation Systems*, *19*(8), 2558–2571. http://dx.doi.org/10.1109/tits.2017.2758343, URL https://doi.org/10.1109%2Ftits.2017.2758343.

Argyropoulos, P. (2003). A semi-empirical model of the direct methanol fuel cell performance part I. Model development and verification. *Journal of Power Sources*, *123*(2), 190–199. http://dx.doi.org/10.1016/s0378-7753(03)00558-5, URL https://doi.org/10.101%2Fs0378-7753%2803%2900558-5.

Automotive Stability Enhancement Systems, (2004). http://dx.doi.org/10.4271/j2564_200406 URL https://doi.org/10.4271%2Fj2564_200406.

Bakker, E., Nyborg, L., & Pacejka, H. B. (1987). Tyre modelling for use in vehicle dynamics studies. In *SAE technical paper series*. SAE International, http://dx.doi.org/10.4271/870421, URL https://doi.org/10.4271%2F870421.

Bakker, E., Pacejka, H. B., & Lidner, L. (1989). A new tire model with an application in vehicle dynamics studies. In *SAE technical paper series*. SAE International, http://dx.doi.org/10.4271/890087, URL https://doi.org/10.4271%2F890087.

Basri, S., & Kamarudin, S. K. (2011). Process system engineering in direct methanol fuel cell. *International Journal of Hydrocarbon Engineering*, *36*(10), 6219–6236. http://dx.doi.org/10.1016/j.ijhydene.2011.02.058, URL https://doi.org/10.1016%2Fj.ijhydene.2011.02.058.

Blundell, M. V. (1999). The modelling and simulation of vehicle handling part 1: Analysis methods. *Proceedings of the Institution of Mechanical Engineers, Part K: Journal of Multi-body Dynamics*, *213*(2), 103–118. http://dx.doi.org/10.1243/1464419991544090, URL https://doi.org/10.1243%2F1464419991544090.

Blundell, M. V. (2000). The modelling and simulation of vehicle handling part 4: Handling simulation. *Proceedings of the Institution of Mechanical Engineers, Part K: Journal of Multi-body Dynamics*, *214*(2), 71–94. http://dx.doi.org/10.1243/1464419001544250, URL https://doi.org/10.1243%2F1464419001544250.

Chan, H. L. (2000). A new battery model for use with battery energy storage systems and electric vehicles power systems. In *2000 IEEE power engineering society winter meeting. conference proceedings (Cat. No.00CH37077)*, IEEE, http://dx.doi.org/10.1109/pesw.2000.850009 URL https://doi.org/10.1109%2Fpesw.2000.850009.

Chiu, Y.-J. (2010). An algebraic semi-empirical model for evaluating fuel crossover fluxes of a DMFC under various operating conditions. *International Journal of Hydrocarbon Engineering*, *35*(12), 6418–6430. http://dx.doi.org/10.1016/j.ijhydene.2010.03.080, URL https://doi.org/10.1016%2Fj.ijhydene.2010.03.080.

Chiu, Y.-J., Yu, T. L., & Chung, Y.-C. (2011). A semi-empirical model for efficiency evaluation of a direct methanol fuel cell. *Journal of Power Sources*, *196*(11), 5053–5063. http://dx.doi.org/10.1016/j.jpowsour.2011.01.084, URL https://doi.org/10.1016%2Fj.jpowsour.2011.01.084.

Dai, Y., Luo, Y., & Li, K. (2013). Longitudinal and lateral coordinated motion control of four-wheel-independent drive electric vehicles. In *2013 world electric vehicle symposium and exhibition (EVS27)*. IEEE, http://dx.doi.org/10.1109/evs.2013.6914736, URL https://doi.org/10.1109%2Fevs.2013.6914736.

Delavar, M. A., Farhadi, M., & Sedighi, K. (2010). Numerical simulation of direct methanol fuel cells using lattice Boltzmann method. *International Journal of Hydrocarbon Engineering*, *35*(17), 9306–9317. http://dx.doi.org/10.1016/j.ijhydene.2010.02.126, URL https://doi.org/10.1016%2Fj.ijhydene.2010.02.126.

Dixon, G., Stobart, R., & Steffen, T. (2015). *Unified backwards facing and forwards facing simulation of a hybrid electric vehicle using MATLAB Simscape*. © SAE International.

Dohle, H., & Wippermann, K. (2004). Experimental evaluation and semi-empirical modeling of u/i characteristics and methanol permeation of a direct methanol fuel cell. *Journal of Power Sources*, *135*(1–2), 152–164. http://dx.doi.org/10.1016/j.jpowsour.2004.04.014, URL https://doi.org/10.1016%2Fj.jpowsour.2004.04.014.

Dowgiallo, E. (1980). *Lead acid battery pulse discharge investigation. Final report, Tech. rep.*. Office of Scientific and Technical Information (OSTI), http://dx.doi.org/10.2172/5080634, URL https://doi.org/10.2172%2F5080634.

Ehsani, M. (2013). Electric, hybrid, and fuel cell vehicles, introduction. In *Transportation technologies for sustainability* (pp. 492–493). Springer New York, http://dx.doi.org/10.1007/978-1-4614-5844-9_915, URL https://doi.org/10.1007%2F978-1-4614-5844-9_915.

Gao, X. (2014). *HT-PEM fuel cell system with integrated thermoelectric exhaust heat recovery : dissertation submittet to the Faculty of Engineering and Science at Aalborg University in partial fulfillment of the requirements for the degree of Doctor of Philosophy* (Ph.D. thesis), Aalborg: Department of Energy Technology, Aalborg University, URL http://www.forskningsdatabasen.dk/en/catalog/2398064122.

Gerdes, J. C., & Hedrick, J. K. (1999). Brake system modeling for simulation and control. *Journal of Dynamic Systems, Measurement, and Control*, *121*(3), 496. http://dx.doi.org/10.1115/1.2802501, URL https://doi.org/10.1115%2F1.2802501.

Graves, C., Ebbesen, S. D., Mogensen, M., & Lackner, K. S. (2011). Sustainable hydrocarbon fuels by recycling CO 2 and H 2 O with renewable or nuclear energy. *Renewable & Sustainable Energy Reviews*, *15*(1), 1–23. http://dx.doi.org/10.1016/j.rser.2010.07.014, URL https://doi.org/10.1016%2Fj.rser.2010.07.014.

Guo, J., Luo, Y., & Li, K. (2018). Adaptive non-linear trajectory tracking control for lane change of autonomous four-wheel independently drive electric vehicles. *IET Intelligent Transport Systems*, *12*(7), 712–720. http://dx.doi.org/10.1049/iet-its.2017.0278, URL https://doi.org/10.1049%2Fiet-its.2017.0278.

Guo, H., & fang Ma, C. (2004). 2d analytical model of a direct methanol fuel cell. *Electrochemistry Communications*, *6*(3), 306–312. http://dx.doi.org/10.1016/j.elecom.2004.01.005, URL https://doi.org/10.1016%2Fj.elecom.2004.01.005.

Haidar, A. M. A., & Muttaqi, K. M. (2015). Behavioral characterization of electric vehicle charging loads in a distribution power grid through modeling of battery chargers. *IEEE Transactions on Industry Applications*, *52*(1), 483–492.

He, H., Xiong, R., Guo, H., & Li, S. (2012). Comparison study on the battery models used for the energy management of batteries in electric vehicles. *Energy Conversion and Management*, *64*, 113–121. http://dx.doi.org/10.1016/j.enconman.2012.04.014, URL https://doi.org/10.1016%2Fj.enconman.2012.04.014.

He, H., Xiong, R., Zhang, X., Sun, F., & Fan, J. (2011). State-of-charge estimation of the lithium-ion battery using an adaptive extended kalman filter based on an improved thevenin model. *IEEE Transactions on Vehicular Technology*, *60*(4), 1461–1469. http://dx.doi.org/10.1109/tvt.2011.2132812, URL https://doi.org/10.1109%2Ftvt.2011.2132812.

Hegazy, S., Rahnejat, H., & Hussain, K. (1999). Multi-body dynamics in full-vehicle handling analysis. *Proceedings of the Institution of Mechanical Engineers, Part K: Journal of Multi-body Dynamics*, *213*(1), 19–31. http://dx.doi.org/10.1243/1464419991544027, URL https://doi.org/10.1243%2F1464419991544027.

Hofman, T., Steinbuch, M., van Druten, R. M., & Serrarens, A. F. A. (2006). Rule-based energy Management strategies for hybrid vehicle drivetrains: a fundamental approach in reducing computation time. *IFAC Proceedings Volumes*, *39*(16), 740–745. http://dx.doi.org/10.3182/20060912-3-DE-2911.00128, URL http://www.sciencedirect.com/science/article/pii/S1474667015342567, 4th IFAC Symposium on Mechatronic Systems.

Hwang, S.-H., Kim, H., Kim, D., & Jung, K. (2010). Analysis of a regenerative braking system for a hybrid electric vehicle using electro-mechanical brakes. In S. Soylu (Ed.), *Urban transport and hybrid vehicles*. Rijeka: IntechOpen, http://dx.doi.org/10.5772/10183, URL https://doi.org/10.5772/10183.

Jaiswal, M., Mavros, G., Rahnejat, H., & King, P. D. (2007). *A multi-body dynamics approach for the study of critical handling manoeuvres on surfaces with uneven friction.*. Delft University of Technology, doi: 9789081176811. URL https://dspace.lboro.ac.uk/2134/14746.

Jaiswal, M., Mavros, G., Rahnejat, H., & King, P. D. (2009). Influence of tyre transience on anti-lock braking. *Proceedings of the Institution of Mechanical Engineers, Part K: Journal of Multi-body Dynamics*, *224*(1), 1–17. http://dx.doi.org/10.1243/14644193jmbd225, URL https://doi.org/10.1243%2F14644193jmbd225.

Jensen, S. H., Sun, X., Ebbesen, S. D., Knibbe, R., & Mogensen, M. (2010). Hydrogen and synthetic fuel production using pressurized solid oxide electrolysis cells. *International Journal of Hydrocarbon Engineering*, *35*(18), 9544–9549. http://dx.doi.org/10.1016/j.ijhydene.2010.06.065, URL https://doi.org/10.1016%2Fj.ijhydene.2010.06.065.

Jimenez, A., & Garcia, N. (2011). Power flow modeling and analysis of voltage source converter-based plug-in electric vehicles. In *2011 IEEE power and energy society general meeting* (pp. 1–6). IEEE.

Ko, J., Chippar, P., & Ju, H. (2010). A one-dimensional, two-phase model for direct methanol fuel cells – part i: Model development and parametric study. *Energy*, *35*(5), 2149–2159. http://dx.doi.org/10.1016/j.energy.2010.01.034, URL https://doi.org/10.1016%2Fj.energy.2010.01.034.

Ko, J., Ko, S., Bak, Y., Jang, M., Yoo, B., Cheon, J., et al. (2013). Development of regenerative braking co-operative control system for automatic transmission-based hybrid electric vehicle using electronic wedge brake. In *2013 world electric vehicle symposium and exhibition (EVS27)* (pp. 1–5). http://dx.doi.org/10.1109/EVS.2013.6914740.

Ko, J., Ko, S., Son, H., Yoo, B., Cheon, J., & Kim, H. (2015). Development of brake system and regenerative braking cooperative control algorithm for automatic-transmission-based hybrid electric vehicles. *IEEE Transactions on Vehicular Technology*, *64*(2), 431–440. http://dx.doi.org/10.1109/TVT.2014.2325056.

Kongjeen, Y., & Bhumkittipich, K. (2016). Modeling of electric vehicle loads for power flow analysis based on PSAT. In *2016 13th international conference on electrical engineering/electronics, computer, telecommunications and information technology (ECTI-CON)* (pp. 1–6). IEEE.

Kortm, W. (1993). Review of multibody computer, codes for vehicle system dynamics. *Vehicle System Dynamics*, *22*(sup1), 3–31. http://dx.doi.org/10.1080/00423119308969463, URL https://doi.org/10.1080%2F00423119308969463.

Kuiper, E., & Oosten, J. J. M. V. (2007). The PAC2002 advanced handling tire model. *Vehicle System Dynamics*, *45*(sup1), 153–167. http://dx.doi.org/10.1080/00423110701773893, URL https://doi.org/10.1080%2F00423110701773893.

Kulikovsky, A. A. (2002). The voltage–current curve of a direct methanol fuel cell: "exact" and fitting equations. *Electrochemistry Communications*, *4*(12), 939–946. http://dx.doi.org/10.1016/s1388-2481(02)00494-0, URL https://doi.org/10.1016%2Fs1388-2481%2802%2900494-0.

Liu, G., Ren, H., Chen, S., & Wang, W. (2013). The 3-DoF bicycle model with the simplified piecewise linear tire model. In *Proceedings 2013 international conference on mechatronic sciences, electric engineering and computer (MEC)*. IEEE, http://dx.doi.org/10.1109/mec.2013.6885617, URL https://doi.org/10.1109%2Fmec.2013.6885617.

Luk, P., & Jinupun, P. (2006). An in-wheel switched reluctance motor for electric vehicles. In *2006 CES/IEEE 5th international power electronics and motion control conference*. IEEE, http://dx.doi.org/10.1109/ipemc.2006.4778329, URL https://doi.org/10.1109%2Fipemc.2006.4778329.

McHenry, R. R. (1969). An analysis of the dynamics of automobiles during simultaneous cornering and ride motions. *Computer-Aided Design*, *1*(3), 19–32. http://dx.doi.org/10.1016/s0010-4485(69)80082-5, URL https://doi.org/10.1016%2Fs0010-4485%2869%2980082-5.

Mller, H., Bernt, A.-O., Salman, P., & Trattner, A. (2017). Fuel cell range extended electric vehicle fcreev long driving ranges without emissions. *ATZ worldwide*, *119*(5), 56–60. http://dx.doi.org/10.1007/s38311-017-0033-0, URL https://doi.org/10.1007%2Fs38311-017-0033-0.

Mohan, G., Assadian, F., & Longo, S. (2013). Comparative analysis of forward-facing models vs backwardfacing models in powertrain component sizing. In *IET hybrid and electric vehicles conference 2013 (HEVC 2013)* (pp. 1–6). http://dx.doi.org/10.1049/cp.2013.1920.

Mutoh, N., Hayano, Y., Yahagi, H., & Takita, K. (2007). Electric braking control methods for electric vehicles with independently driven front and rear wheels. *IEEE Transactions on Industrial Electronics*, *54*(2), 1168–1176. http://dx.doi.org/10.1109/TIE.2007.892731, URL https://doi.org/10.5772/10183.

Naayagi, R., & Kamaraj, V. (2005). A Comparative Study of Shape Optimization of SRM using Genetic Algorithm and Simulated Annealing. In *2005 annual IEEE India conference - INDICON*, IEEE, http://dx.doi.org/10.1109/indcon.2005.1590241 URL https://doi.org/10.1109%2Findcon.2005.1590241.

Norouzi, A., Kazemi, R., & Azadi, S. (2017). Vehicle lateral control in the presence of uncertainty for lane change maneuver using adaptive sliding mode control with fuzzy boundary layer. *Proceedings of the Institution of Mechanical Engineers, Part I: Journal of Systems and Control Engineering*, *232*(1), 12–28. http://dx.doi.org/10.1177/0959651817733222, URL https://doi.org/10.1177%2F0959651817733222.

Pacejka, H. B. (2012). Preface. In *Tire and vehicle dynamics* (pp. xiii–xvi). Elsevier, http://dx.doi.org/10.1016/b978-0-08-097016-5.05001-4, URL https://doi.org/10.1016%2Fb978-0-08-097016-5.05001-4.

Pacejka, H. B., & Besselink, I. J. M. (1996). Magic formula tyre model with transient properties. *Vehicle System Dynamics*, *27*, 234–249. http://dx.doi.org/10.1080/00423119608969658, URL https://doi.org/10.1080%2F00423119608969658.

Plett, G. L. (2004). Extended kalman filtering for battery management systems of lipb-based HEV battery packs. *Journal of Power Sources*, *134*(2), 252–261. http://dx.doi.org/10.1016/j.jpowsour.2004.02.031, URL https://doi.org/10.1016%2Fj.jpowsour.2004.02.031.

Pofahl, S. N. (2012). *Modeling the direct methanol fuel cell* (Ph.D. thesis), Universität Ulm, http://dx.doi.org/10.18725/OPARU-2585, URL https://oparu.uni-ulm.de/xmlui/handle/123456789/2612.

Pop, C. V., & Fodorean, D. (2016). In-wheel motor with integrated magnetic gear for extended speed applications. In *2016 international symposium on power electronics, electrical drives, automation and motion (SPEEDAM)*. IEEE, http://dx.doi.org/10.1109/speedam.2016.7525873, URL https://doi.org/10.1109%2Fspeedam.2016.7525873.

Rajamani, R. (2011). Longitudinal vehicle dynamics. In *Mechanical engineering series* (pp. 87–111). Springer US, http://dx.doi.org/10.1007/978-1-4614-1433-9_4, URL https://doi.org/10.1007%2F978-1-4614-1433-9_4.

Ren, H., Shim, T., Ryu, J., & Chen, S. (2014). Development of effective bicycle model for wide ranges of vehicle operations. In *SAE technical paper series*. SAE International, http://dx.doi.org/10.4271/2014-01-0841, URL https://doi.org/10.4271%2F2014-01-0841.

Rizzoni, G., Guzzella, L., & Baumann, B. M. (1999). Unified modeling of hybrid electric vehicle drivetrains. *IEEE/ASME Transactions on Mechatronics*, *4*(3), 246–257.

Salameh, Z. M., Casacca, M. A., & Lynch, W. A. (1992). A mathematical model for lead-acid batteries. *IEEE Transactions on Energy Conversion*, *7*(1), 93–98. http://dx.doi.org/10.1109/60.124547, URL https://doi.org/10.1109%2F60.124547.

Shabana, A. A. (2009). *Dynamics of multibody systems*. Cambridge University Press, http://dx.doi.org/10.1017/cbo9781107337213, URL https://doi.org/10.1017%2Fcbo9781107337213.

Shankar, R., Marco, J., & Carroll, S. (2011). Performance of an EV during real-world usage. In *Cenex hybrid electric vehicle conference*. UK.

Soylu, S. (Ed.), (2011). *Electric vehicles - modelling and simulations*. InTech, http://dx.doi.org/10.5772/958, URL https://doi.org/10.5772%2F958.

Suh, I.-S., Hwang, K., Lee, M., & Kim, J. (2013). In-wheel motor application in a 4wd electric vehicle with foldable body concept. In *2013 International electric machines & drives conference*. IEEE, http://dx.doi.org/10.1109/iemdc.2013.6556292, URL https://doi.org/10.1109%2Fiemdc.2013.6556292.

Sun, W., Li, Y., Huang, J., & Zhang, N. (2015). Vibration effect and control of in-wheel switched reluctance motor for electric vehicle. *Journal of Sound and Vibration*, *338*, 105–120. http://dx.doi.org/10.1016/j.jsv.2014.10.036, URL https://doi.org/10.1016%2Fj.jsv.2014.10.036.

Sundmacher, K., Schultz, T., Zhou, S., Scott, K., Ginkel, M., & Gilles, E. D. (2001). Dynamics of the direct methanol fuel cell (DMFC): experiments and model-based analysis. *Chemical Engineering Science*, *56*(2), 333–341. http://dx.doi.org/10.1016/s0009-2509(00)00233-5, URL https://doi.org/10.1016%2Fs0009-2509%2800%2900233-5.

Vehicle Dynamics Terminology, (2008). http://dx.doi.org/10.4271/j670_200801 URL https://doi.org/10.4271%2Fj670_200801.

Wang, W., & Fahimi, B. (2012). Comparative study of electric drives for EV/HEV propulsion system. In *2012 electrical systems for aircraft, railway and ship propulsion*. IEEE, http://dx.doi.org/10.1109/esars.2012.6387497, URL https://doi.org/10.1109%2Fesars.2012.6387497.

Wang, Y., Li, P., & Ren, G. (2016). Electric vehicles with in-wheel switched reluctance motors: Coupling effects between road excitation and the unbalanced radial force. *Journal of Sound and Vibration*, *372*, 69–81. http://dx.doi.org/10.1016/j.jsv.2016.02.040, URL https://doi.org/10.1016%2Fj.jsv.2016.02.040.

yang Wang, Y., & ning Yang, F. (2017). SRM representative parameters effect on in-wheel motored vehicle performance. In *2017 2nd IEEE international conference on intelligent transportation engineering (ICITE)*. IEEE, http://dx.doi.org/10.1109/icite.2017.8056877, URL https://doi.org/10.1109%2Ficite.2017.8056877.

Wang, Y., Yu, S., Yuan, J., & Chen, H. (2018). Fault-tolerant control of electric ground vehicles using a triple-step nonlinear approach. *IEEE/ASME Transactions on Mechatronics*, *23*(4), 1775–1786. http://dx.doi.org/10.1109/tmech.2018.2837128, URL https://doi.org/10.1109%2Ftmech.2018.2837128.

Wang, Y., Zheng, J. P., Au, G., & Plichta, E. J. (2008). A semi-empirical method for electrically modeling of fuel cell: executed on a direct methanol fuel cell. In *ECS transactions*. ECS, http://dx.doi.org/10.1149/1.2921549, URL https://doi.org/10.1149%2F1.2921549.

de Wit, C. C., & Tsiotras, P. (1999). Dynamic tire friction models for vehicle traction control. In: *Proceedings of the 38th IEEE conference on decision and control (Cat. No.99CH36304)*, IEEE, http://dx.doi.org/10.1109/cdc.1999.827937 URL https://doi.org/10.1109%2Fcdc.1999.827937.

Wood, E., Wang, L., Gonder, J., & Ulsh, M. (2013). Overcoming the range limitation of medium-duty battery electric vehicles through the use of hydrogen fuel-cells. *SAE International Journal of Commercial Vehicles*, *6*(2), 563–574. http://dx.doi.org/10.4271/2013-01-2471, URL https://doi.org/10.4271%2F2013-01-2471.

Xu, W., Chen, H., Zhao, H., & Ren, B. (2019). Torque optimization control for electric vehicles with four in-wheel motors equipped with regenerative braking system. *Mechatronics*, *57*, 95–108. http://dx.doi.org/10.1016/j.mechatronics.2018.11.006, URL http://www.sciencedirect.com/science/article/pii/S0957415818301752.

Xu, L., & Xiao, J. (2011). Modeling and simulation of PEM fuel cells based on electrochemical model. In *2011 international conference on remote sensing, environment and transportation engineering*. IEEE, http://dx.doi.org/10.1109/rsete.2011.5964316, URL https://doi.org/10.1109%2Frsete.2011.5964316.

Ye, C., Miao, S., Lei, Q., & Li, Y. (2016). Dynamic energy management of hybrid energy storage systems with a hierarchical structure. *Energies*, *9*(6), 395. http://dx.doi.org/10.3390/en9060395, URL https://doi.org/10.3390%2Fen9060395.

Yin, G., Chen, N., & Li, P. (2007). Improving handling stability performance of four-wheel steering vehicle via μ-synthesis robust control. *IEEE Transactions on Vehicular Technology*, *56*(5), 2432–2439. http://dx.doi.org/10.1109/tvt.2007.899941, URL https://doi.org/10.1109%2Ftvt.2007.899941.

Yu, S., Wang, J., Wang, Y., & Chen, H. (2018). Disturbance observer based control for four wheel steering vehicles with model reference. *IEEE/CAA Journal of Automatica Sinica*, *5*(6), 1121–1127. http://dx.doi.org/10.1109/JAS.2016.7510220.

Zaidy, A., Pokharkar, P., Krishnan, R., & Sonawane, D. (2014). Dynamic modeling and simulation of a PEM fuel cell: MATLAB and labview modeling approach. In *2014 1st international conference on non conventional energy (ICONCE 2014)*. IEEE, http://dx.doi.org/10.1109/iconce.2014.6808744, URL https://doi.org/10.1109%2Ficonce.2014.6808744.

Zou, J., He, Y., Miao, Z., & Li, X. (2010). Non-isothermal modeling of direct methanol fuel cell. *International Journal of Hydrocarbon Engineering*, *35*(13), 7206–7216. http://dx.doi.org/10.1016/j.ijhydene.2010.01.123, URL https://doi.org/10.1016%2Fj.ijhydene.2010.01.123.